Biomedical Uses for 2D Materials Beyond Graphene: Current Advances and Challenges Ahead

*Rajendra Kurapati, Kostas Kostarelos, Maurizio Prato, and Alberto Bianco**

Currently, a broad interdisciplinary research effort is pursued on biomedical applications of 2D materials (2DMs) beyond graphene, due to their unique physicochemical and electronic properties. The discovery of new 2DMs is driven by the diverse chemical compositions and tuneable characteristics offered. Researchers are increasingly attracted to exploit those as drug delivery systems, highly efficient photothermal modalities, multimodal therapeutics with non-invasive diagnostic capabilities, biosensing, and tissue engineering. A crucial limitation of some of the 2DMs is their moderate colloidal stability in aqueous media. In addition, the lack of suitable functionalisation strategies should encourage the exploration of novel chemical methodologies with that purpose. Moreover, the clinical translation of these emerging materials will require undertaking of fundamental research on biocompatibility, toxicology and biopersistence in the living body as well as in the environment. Here, a thorough account of the biomedical applications using 2DMs explored today is given.

1. Introduction

The isolation and discovery of the extraordinary properties of graphene have become a strong motive in the search of new two-dimensional materials (2DMs) exhibiting different optical, electrical and thermal properties.[1,2] 2DMs are currently intensively investigated as alternative to graphene-based materials,[3,4] and in their planar form show unique physicochemical properties, particularly associated to the high electronic and thermal conductivity.[5] The family of 2DMs comprises different chemical classes, the most popular of which include 2D layered transition-metal dichalcogenides (TMDCs), transition metal dioxides (TMDOs), hexagonal boron nitride (hBN), graphitic C_3N_4 (g-C_3N_4), 2D clay materials, such as layered double hydroxides (LDHs) and laponite (LAP), and the recent member consisting of ultra-thin black phosphorous (BP) monolayers.[6–9] These types of materials are finding numerous applications in electronics, optoelectronics, energy storage, sensors and catalysis,[10] but also hold great potential in the biomedical field.[8,11,12] Indeed, it is possible to obtain stable aqueous dispersions under physiological conditions with 2DMs, either by chemical functionalisation or coating with surfactants to favor interactions with living systems. Towards this direction, these materials represent a great alternative for the development of the next generation of tools for biomedical applications, potentially surpassing the performance of carbon-based nanomaterials (i.e., carbon nanotubes, nanohorns, graphene, carbon dots, etc.). This can be due to the possibility of tuning their electronic and optical properties, exploiting their surface area for combination with other molecules or materials, and insertion of chemical modifications by appropriate functionalisation strategies.[13]

2D transition metal dichalcogenides, transition metal oxides, and g-C_3N_4 are being intensively explored as field-effect transistors (FETs), gas sensors, including biosensors, and in bioimaging due to their wide direct band-gap compared to that of their bulk form.[2,14] On the other hand, TMDCs have been applied for potential applications in photothermal therapy (PTT) along with multimodal imaging guidance for treating tumours due to their unique optical properties.[15] hBN (known as "white graphene") is also widely explored as alternative to graphene. Although hBN nanosheets act as pure insulators and do not absorb light in the visible light region, they have received increasing attention due to their superior mechanical strength, thermal conductivity, low fluorescence quenching along with chemical inertness over other 2DMs.[16–19] They have been used to improve the mechanical and thermal properties of polymer composites and high-temperature oxidation-resistance coatings.[16,18,20,21] In addition, functionalised hBN nanosheets have been also used in biomedical applications such as bioimaging due to their excellent water dispersibility combined with very low cellular toxicity.[22] However, there are very few reports

Dr. R. Kurapati, Dr. A. Bianco
CNRS
Institut de Biologie Moléculaire et Cellulaire
Laboratoire d'Immunopathologie
et Chimie Thérapeutique
67000 Strasbourg, France
E-mail: a.bianco@ibmc-cnrs.unistra.fr
Prof. K. Kostarelos
Nanomedicine Laboratory
School of Medicine and National Graphene Institute
University of Manchester
AV Hill Building, Manchester M13 9PT, United Kingdom
Prof. M. Prato
Dipartimento di Scienze Chimiche e Farmaceutiche
Università di Trieste, 34127 Trieste, Italy
Prof. M. Prato
Carbon Nanobiotechnology Laboratory
CIC biomaGUNE
Donostia-San Sebastian, Paseo de Miramón 182, 20009, Spain
Prof. M. Prato
Basque Foundation for Science (IKERBASQUE)
Bilbao 48013, Spain

DOI: 10.1002/adma.201506306

on the biomedical application of BNs, therefore more studies are needed to explore their potential in biomedicine.[22]

The g-C_3N_4 nanosheets also hold promising characteristics such as water dispersibility without addition of any surfactants or oxidation treatments as seen for other 2DMs (TMDCs or graphene-based materials). Indeed, g-C_3N_4 can be easily exfoliated directly in aqueous solutions.[23] Moreover, graphitic C_3N_4 sheets exhibit a large band-gap similar to TMDCs as well as superior photocatalytic features ranging from UV to visible region, thereby finding applications in biosensing, bioimaging, drug delivery and photothermal therapy.[24–26] Graphene analogues such as MoS_2 and g-C_3N_4 display large band-gaps compared to graphene, which can be tuned between semiconductor or insulator forms in a controlled manner,[27] preventing current leakage and allowing higher sensitivity and accuracy of readings.[28] Very recently, metal-free layers made of black phosphorous, displaying thickness-dependent band-gap is attracting the interest of researchers.[29] Applications in electronics and optoelectronics started to be investigated.[30] However, compared to other 2DMs, bioapplications are still rudimentary due to the lack of suitable exfoliation methods. BP nanosheets were shown to generate singlet oxygen species under the entire visible light region and applied for photodynamic therapy to treat tumours in mouse models.[6,31] The family of 2D clay materials, including LDHs and LAP nanodiscs, holds interesting biomedical possibilities, especially in drug delivery. These materials allow a sustained drug release, the delivery of hydrophobic molecules, and they are highly biocompatible.[7,32] They resulted also useful in tissue engineering and as antimicrobial coatings.[33–35]

Some initial reports showed reduced levels of cytotoxicity for the different 2DMs mentioned above compared to other nanomaterials.[6,22,26,36,37] The low cytotoxicity of 2DMs have been postulated to be due to the lack of sharp edges (e.g., MoS_2 sheets) compared to graphene-based materials.[38,39] These 2DMs have been also described to possess material-type dependent antimicrobial properties similar to those reported for graphene or graphene oxide.[40,41] However, all such reports are too preliminary to reach any validated conclusions.

The assessment of the health and environmental impact from exposure to 2DMs is certainly facilitated by their chemical nature and composition. While it is quite challenging to track the fate of carbon nanomaterials quantitatively, necessitating their labelling in order to distinguish them from endogenous carbon, the metallic composition of TMDCs and LDHs may allow a much more facile detection at the cellular, tissue and organ level.

In view of the promising characteristics of 2DMs for biology and medicine, in this review article we will outline the possibilities offered in some of these applications. We will not cover graphene-based materials, as they have been recently extensively described in many interesting and exhaustive reviews.[42–54] In addition, to clearly diversify our contribution from other recent reviews,[55] we have organized the sections not based on the type of material but on the different biomedical applications to highlight their emerging importance in biomedicine. We will describe in particular the use of 2DMs in therapy, imaging and diagnosis (**Figure 1**). A brief section will initially discuss the main methods used to prepare these materials. We will finally cover aspects related to knowledge generated on safety and toxicity of 2DMs and provide future perspectives.

Alberto Bianco received his PhD in 1995 from the University of Padova (Italy). As a visiting scientist, he worked at the University of Lausanne, Tübingen (as an Alexander von Humboldt fellow) and Padova. He is currently Research Director at the CNRS in Strasbourg. His research interests focus on the design and functionalisation of carbon-based nanomaterials (carbon nanotubes, graphene and adamantane) for therapeutic, diagnostic and imaging applications. He is co-author of over 200 papers.

2. Synthetic Methods and Surface Functionalization

The preparation of 2D layered nanomaterials can be achieved using two distinct methods: i) the top-down approach; and ii) the bottom-up approach. Both have been extensively covered in recent reviews.[3,5,56,57] In this section, we will briefly summarise the main differences between these two approaches. In addition, we will also underline the importance of modulating the surface chemistry of 2DMs for biomedical applications by adding appropriate functionalization groups necessary to render them compatible with biological (i.e., cells and tissues) and living systems (i.e., animal models) (**Figure 2**).

The top-down method is based on the direct exfoliation of bulk material. Exfoliation covers alternative possibilities including mechanical treatments, ion intercalation, liquid-phase and surfactant-assisted exfoliation/dispersion. By applying these processes, almost all types of 2D materials can be obtained as single-, few- or multi-layered nanosheets in different solvents including water and physiological solutions. Among the different exfoliation processes listed above, the liquid-phase can be considered the most efficient and versatile as it allows preparation of large amounts of any materials,[58] particularly suited for biomedical purposes.[12] This method can also produce specific surface functionalizations that are particularly advantageous to stabilise the nanosheets in solution.[59–63] Generally, modifications of 2DM surfaces introduce defects that can affect the electronic properties. However, these defects are fundamental for further chemical functionalisation and tuning material characteristics.[61,62,64]

The bottom-up method is the alternative process to generate 2D layered materials via atomic level control of their composition and structure. It can be used to synthesise 2DMs that cannot be obtained by direct exfoliation from bulk. Chemical vapor deposition (CDV) growth and wet chemical synthesis allow preparation of size-controlled and chemically pure materials. Between these two bottom-up processes, the second is the

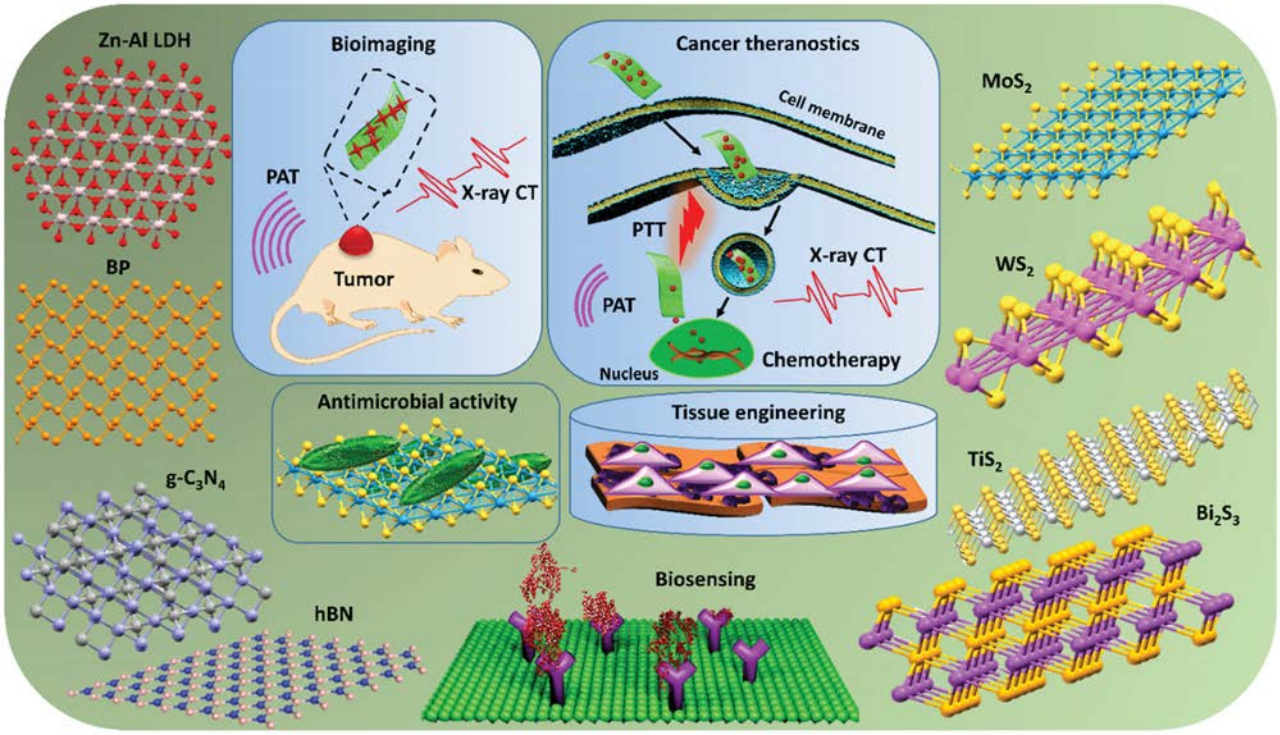

Figure 1. Molecular structures and biomedical opportunities offered by 2DMs.

more versatile, as CVD is limited by the choice of an appropriate substrate to grow the desired material, high temperature and high vacuum conditions, followed by the requirement of its final removal from the substrate.[65] In general, the CVD method is suitable to grow single-crystalline 2D sheets for device fabrication, but less appropriate for biomedical applications.[12,33] Wet chemistry is instead particularly useful for layered hydroxide-like materials where the fine control of the composition and the ratio between single atoms are fundamental to endow these materials with the desired properties.[33] Wet chemistry starting from the appropriate reagents can be also exploited to synthesise novel hybrid materials, like carbon-doped hBN or metal ion-doped WS_2 sheets.[66,67]

In the biomedical field it is of paramount importance to maintain any materials stable in solution. Most of 2DMs suffer from rapid reaggregation and precipitation in

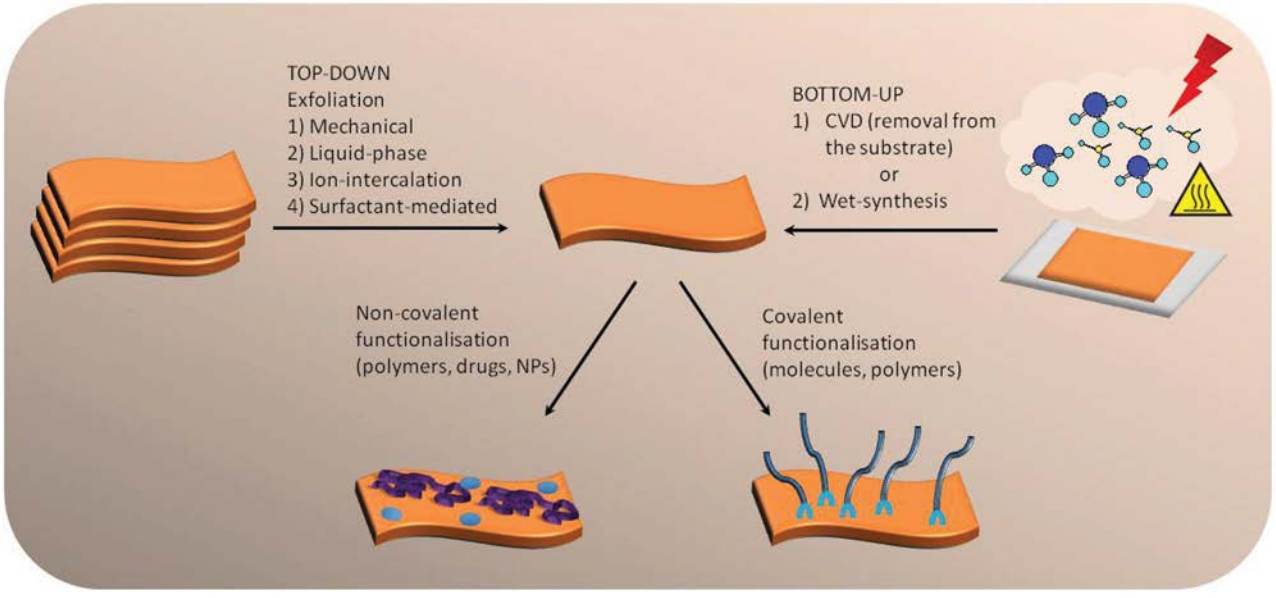

Figure 2. Schematic representation of the synthetic methods to obtain multifunctional 2D materials.

physiological conditions. Chemical functionalisation is therefore essential to endow the nanomaterial with high colloidal stability. In addition, the functionalisation can also impart targeting characteristics that can allow localisation of conjugates with therapeutic activity into the tumour for cancer treatment. Functionalisation can be non-covalent when surfactants or polymers are used to disperse the nanosheets, or covalent if an appropriate function reacts with the surface atoms of the 2DMs (Figure 2). For example, the covalent functionalisation of MoS_2 has been very recently described by Presolski and Pumera.[63] The advantage of this method resides in the chemical stability of the bond between the nanomaterial and the functional molecule.[68] The most explored molecule to obtain homogenous aqueous dispersions with any 2DMs is polyethylene glycol (PEG). In this case the polymer was mainly physisorbed onto the 2D surface. PEG can potentially offer further benefits as it can also prolong blood circulation of the nanosheets.[39] Alternatively, bovine serum albumin was also exploited for the preparation of homogenous and stable dispersions of 2D crystals.[69] The following sections that describe different biomedical applications of 2DMs will also cover the specific functionalisation strategies and multiple functionalisation approaches performed today. The combination of 2D materials with different nanoparticles also will permit further expansion of their capabilities and applications towards development of novel multimodal technologies for diagnostics or therapeutic applications.

3. Biomedical Applications using 2DMs

3.1. In Vitro and In Vivo Anticancer Applications

Different 2DMs are finding interesting applications in the therapy of cancer as they can combine the capability to deliver a drug and to undergo photothermal induced release of the drug under irradiation in the near infrared (NIR) region, as summarised in **Table 1**. PEGylated MoS_2 has been used to deliver anticancer drugs in an approach combining photothermal ablation and chemotherapy.[68] Following chemical exfoliation, MoS_2 nanosheets were stabilised in water by lipoic acid conjugated PEG (LA-PEG) and loaded with doxorubicin (Dox), Ce6 and an analogue of camptothecin (SN38) reaching very high amounts of drug loading on the sheet surface (>200% in weight). The PEG chain was also modified with folic acid (FA) as the targeting ligand. The complex demonstrated efficient targeting to KB cells (that overexpress folate receptors) in comparison to HeLa cells. Following the uptake of the MoS_2 nanosheets loaded with Dox, the cells that were irradiated with NIR laser light were ablated to a large extent. The biological activity was enhanced by the synergistic combination of the drug action and the NIR irradiation. Combination of chemotherapy and photothermal therapy was also applied in vivo. The complexes of MoS_2 were administered to mice either intratumorally or intravenously. Both routes of administration led to high accumulation of the targeted PEGylated MoS_2 into the tumour site. Tumour growth was significantly inhibited by the synergistic effect of Dox treatment and laser irradiation.

Besides the combination with anticancer drugs, exfoliated MoS_2 can be used alone as a NIR photothermal agent.[70,83] In vitro experiments on HeLa cells demonstrated the photothermal ablative activity under irradiation at 808 nm, leading to complete cell killing. More recently, Shi and co-workers reported a novel and efficient one-pot synthesis of PEG-MoS_2 nanosheets via the bottom-up approach starting from ammonium molybdate and thiourea.[39] This original method allowed control of the size, crystallinity and enhancement of the colloidal stability of PEG-MoS_2. In turn, the photothermal performance was optimised based on the size and PEGylation of the sheets. In vitro viability tests on 4T1 and L929 cells revealed low cytotoxicity of this 2DM, while under laser irradiation at 808 nm cells showed a dose-dependent apoptosis. Highly efficient in vivo photothermal activity was then achieved in a tumour-bearing mouse xenograft model. This work clearly highlights the potential application of MoS_2 sheets for NIR-mediated photothermal therapy.

NIR photothermal properties are intrinsic to all elements of metallic nature, so alternatively to metal-transition dichalcogenides, other noble metals can be obtained in the form of nanosheets and exploited for cancer photothermal ablation. Ultra-small palladium sheets with size below 10 nm were modified with glutathione and administered to tumour-bearing mice.[71] The long blood circulation of this material allowed high accumulation in the tumour. Following laser irradiation at 808 nm, the tumour growth was significantly inhibited.

More recently, metal-free black phosphorous monolayered sheets have also been obtained by direct exfoliation in aqueous medium without use of any surfactants (**Figure 3**). These sheets were stable up to 2 weeks without any degradation of the sheets in the dark.[6] Importantly, these monolayer BP sheets were found to be highly efficient photosensitizers, resulting in generation of singlet oxygen under the entire visible light region, with quantum yields much higher than those reported for established photodynamic therapy (PDT) agents.[84] These BP sheets were injected in Balb/c nude mice intratumorally, followed by 660 nm laser irradiation of the tissue. Tumour growth was significantly reduced in BP sheets-treated mice compared to untreated animals, indicating the potential use of this material for in vivo PDT. In addition, these BP sheets could be degraded readily into biocompatible phosphorous oxides by short-time light irradiation. This is a unique property of BP that has not been reported for other 2DMs. In another study, BP quantum dots (QDs) exhibited excellent biocompatibility, non-immunogenicity, long blood circulation time and were employed instead for PTT.[31]

Within the 2DMs, hBN nanosheets have also been proposed as drug delivery systems for anticancer therapy. hBN has been rendered highly water soluble by functionalisation with hydroxyl groups,[22] making this material capable to efficiently complex Dox. Once added to prostate cancer cells, the drug was released from the nanosheets, affecting cell viability in a dose-dependent manner, and with more efficacy than the drug alone. Further studies are necessary to determine the biological activity of these constructs in in vivo disease models.

In addition to the different 2DMs reported above, LDHs and laponite, a synthetic type of silicate nanodiscs, have also emerged as

Table 1. In vitro and in vivo applications for anticancer therapy and regenerative medicine.

Material	Functionalisation/ Coating	Drug	Modality	In vitro	In vivo	Toxicity effects	Ref.
MoS_2	LA-PEG, Folic acid	Dox, Ce6, SN38	PTT and Chemotherapy	HeLa, KB cells	Mice	No cytotoxic effects after 24 h even at high concentration Induction of minimal oxidative stress	[68]
MoS_2	Intracellular protein complexation		PTTHost-guest protein interaction & enzyme inhibition under NIR light	HeLa		No cytotoxicity without light irradiation Reversible inhibition of enzymatic activity	[70]
MoS_2	PEG	–	PTT	4T1 L929	Mice	Biocompatible up to 500 μg/mL Hemocompatibility After 40 days, Mo level in liver, spleen, lungs was reduced	[39]
Pd sheets	Reduced glutathione	–	Photothermal ablation under NIR irradiation	–	Mice	Long blood circulation Renal clearance Low organ accumulation No organ damage No body weight changes	[71]
BP sheets	–	–	PDT in Visible light	MDA-MB-231 cells	Mice	Biocompatibility, tumor growth inhibition	[6]
Porous hBN and $BN(OH)_x$	Hydroxylation	Dox	Drug delivery	NIH/3T3 LNCaP	–	No cell mortality without drug	[22]
Mg-Al LDH	–	MTX	Drug delivery	HOS and MTX-resistant cells	–	Bypassed MTX resistance, prevented cell proliferation	[72]
LAP	–	Dox	Drug delivery	KB cells	Mice	Enhanced cellular uptake of LAP/Dox No changes in body weight No damage of the organs	[7,73]
LAP	Folic acid PEG-lactobionic acid	Dox	Drug delivery	HeLa L929 cells HepG2	–	FA enhanced anticancer activity	[74,75]
LAP	PEG-poly(lactic acid) copolymer	Dox	Drug delivery	CAL-72	–	Cytocompatibility	[76]
Ti-Ni LDH & $Ni(OH)_2$ films	–	–	Tissue engineering, ROS generation, pH dependent nickel uptake	RBE, HIBEpic, SMMC-7721, HepG2	–	Normal cell proliferation	[77]
MoS_2 (0.01 – 0.2%)	Polypropylene fumarate	–	Bone tissue engineering	–	–	Biocompatible scaffolds, but biodegradation products are cytotoxic	[78,79]
LAP	PLGA nanofibers	–	Bone tissue engineering	hMSCs L929 fibroblasts	–	Hemocompatible, Cytocompatible Biodegradability	[80]
LAP	Bioceramics	–	Bone tissue engineering	Pig RBCs rMSCs	Mice	Hemocompatibility Cytocompatibility	[33]
LAP	Gelatine methacrylate hydrogel	–	Bone tissue engineering	MC3T3 cells	–	Improved cell adhesion, biocompatibility, induced biomineralisation	[81,82]

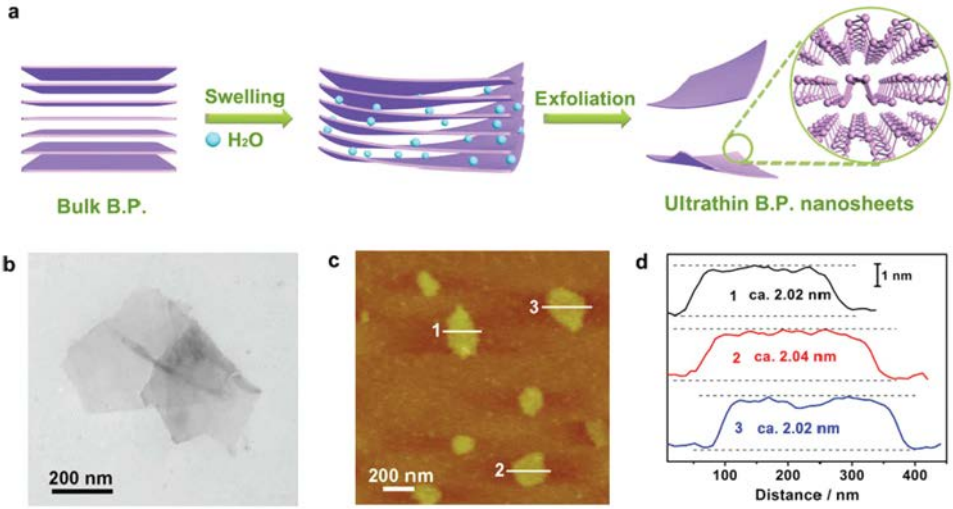

Figure 3. Preparation and morphology of ultrathin BP nanosheets (a) Schematic illustration for the water exfoliation of bulk BP into ultrathin nanosheets. (b) Transmission electron microscopy (TEM) image. (c) Atomic force microscopy image. (d) Corresponding height image. Reproduced with permission.[6] Copyright 2015, American Chemical Society.

novel drug delivery carriers. LDHs have been proposed in drug delivery because of many atomic combinations and high biocompatibility that can result in diverse compositions. Drugs or biomolecules can then be intercalated in LDH layers resulting in a unique drug carrier with high drug loading.[85,86] LDHs, of generic formula $[M^{2+}_{1-x}M^{3+}_{x}(OH)_2][A^{n-}_{x/n}\cdot zH_2O$ (M = di- or trivalent metal cations, and A = interlayer anions) consist of an outer positively charged metal hydroxide sheet and of an inner interlayer of hydrated anions favoring cell internalisation.[32,85,87,88] For instance, methotrexate (MTX) intercalated into a LDH hybrid inhibited cell proliferation in MTX-resistant cells due to an improved permeability and retention effect of LDH-MTX system.[72]

Alternatively, smectite clay laponite resulted in an interesting system for delivery of anticancer drugs because of the high encapsulation efficiency it exhibited.[34,89–91] A novel anticancer therapy exploiting the incorporation of Dox into the interlayer space of LAP (98.3% encapsulation efficiency) via an ionic exchange process has been reported.[7] In vitro drug release studies showed that Dox liberation from LAP was pH-dependent. Cytotoxic assay using human epithelial carcinoma KB cells revealed that LAP/Dox nanodiscs caused higher cytotoxicity than free Dox at the same concentration because of better cellular uptake of the nanodiscs. The antitumour activity of LAP/Dox system was then carried out using a tumour-bearing mouse model.[73] In vivo biodistribution studies also allowed demonstration of the biodegradability of such material. A higher amount of magnesium ions were measured in the organs of the reticuloendothelial systems (RES) (mainly the liver) compared to other organs. After 45 days, the amount of magnesium was negligible revealing that LAP was easily eliminated. Moreover, no organ damage was observed as revealed by histological studies. Recently, the covalent functionalisation of LAP nanodiscs with folic acid, to target cancer cell lines over-expressing folate receptor, was achieved.[74] Similarly, the functionalisation of LAP with PEG-linked lactobionic acid allowed to specifically target human liver HepG2 cancer cells.[75] Further, modifications of LAP with PEG-poly(lactic acid) copolymer improved the aqueous colloidal stability of Dox loaded LAP.[76] All these reports, and in particular the pilot in vivo antitumor studies using LAP/Dox complexes,[73] revealed the exceptional anticancer therapeutic potential of LAPs.

3.2. Tissue Engineering Applications

2DMs have been explored in tissue engineering and regenerative medicine applications since they can offer greater added functionality to polymers due to their large surface area and good mechanical strength (Table 1).[47,92] For example, stents based on nickel and titanium are currently developed for the inhibition of cancer cell proliferation in different organs. Indeed, integration of $Ni(OH)_2$ and Ni-Ti double-layered hydroxide on currently available nickel and titanium alloys can lead to new surfaces with better inhibition rate of cancer cells and improved biocompatibility with normal cells (**Figure 4**).[77] The mechanism of action is based on the release and uptake of nickel ions into the cells with a consequent induction of high level of reactive oxygen species. This effect on normal cells is reportedly reduced; therefore a selective inhibition effect is hypothesised to be dependent on the reversed pH gradient in cancer cells. Again, such observations need to be verified by further studies and most importantly in vivo studies will be necessary.

A recent report showed that a hybrid material made of biodegradable polypropylene fumarate (PPF) and MoS_2 sheets (0.01 – 0.2%) provided greater mechanical strength in bone tissue engineering than multi-walled carbon nanotubes (CNTs) or graphene oxide with the same respective weight ratio.[78] Additional results on the in vivo biocompatibility of the 2DM reinforced polymer scaffolds and their ability to promote osteogenic differentiation are needed to prove their safe use for bone regeneration. In this direction, the functionalisation of 2DMs with various biomolecules to modulate their toxicity or to control biodistribution should be explored. Indeed, their

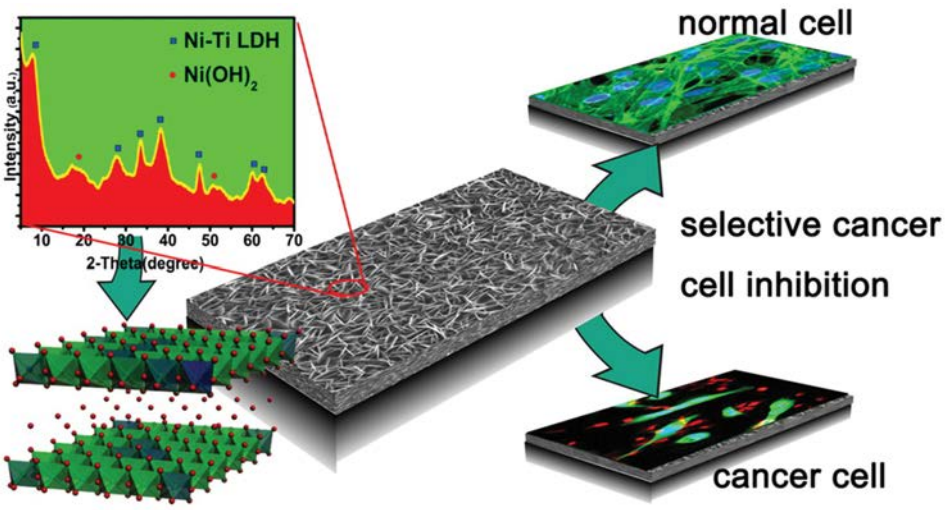

Figure 4. Schematic representation of films composed of $Ni(OH)_2$ or Ni–Ti layered double hydroxide (Ni-Ti LDH) on the top of a surface of nickel and titanium alloy. The films with specific Ni/Ti ratios release a large amount of nickel ions under acidic environments leading to inhibition of cancer cell proliferation while showing little effects to normal cells. Reproduced with permission.[77] Copyright 2015, American Chemical Society.

interactions with various tissues and the potential pro-inflammatory responses to such materials are still unknown. In addition, it is essential to examine the properties of metallic and semiconducting 2DMs to understand how the tissues can benefit of the difference in electron transfer and charge transport.[8]

The inorganic bioceramics consisting of Ca and Mg silicates have been used in bone and tissue engineering for many years, mainly because of their ability to stimulate cell proliferation, differentiation, osteogenic expression and regeneration of bone cells.[33] Along the same direction, the inorganic layered materials such as LAPs and LDHs have also shown some promising results in tissue engineering.[77,80] Especially, LAP-based materials have been shown to offer unique advantages similar to bioactive glass in bone and tissue engineering due to their high biocompatibility, biodegradation into non-toxic products [i.e., Na^+, $Si(OH)_4$, Mg^{2+}, and Li^+], and osteoinduction.[90,80] LAP-doped nanofibers from poly(lactic-*co*-glycolic acid) (PLGA) displayed improved cell adhesion and proliferation of L929 mouse fibroblasts and porcine iliac artery endothelial cells compared to PLGA fibers alone.[80] Importantly, LAP-PLGA scaffolds also induced osteogenic differentiation of human mesenchymal stem cells (hMSCs) without stimulation factors.

Zhao et al. have further demonstrated the applicability of LAP for bone regeneration.[33] A LAP-based bioceramic, prepared by sintering LAP powder, showed an excellent surface hydrophilicity and serum adsorption capacity. An in vitro haemolysis assay using pig red blood cells (RBCs) revealed that the LAP bioceramic exhibited excellent hemocompatibility, a key parameter for tissue engineering. In addition, the LAP bioceramic showed good cytocompatibility on rat mesenchymal stem cells (rMSCs). This composite was able to induce the biomineralisation of hydroxyapatite on its surface after 7 days in stimulated body fluid.[93] It regulated the osteogenic differentiation of rMSCs (**Figure 5**a) without any inducing factors compared to cells cultured onto uncoated tissue cultured plates

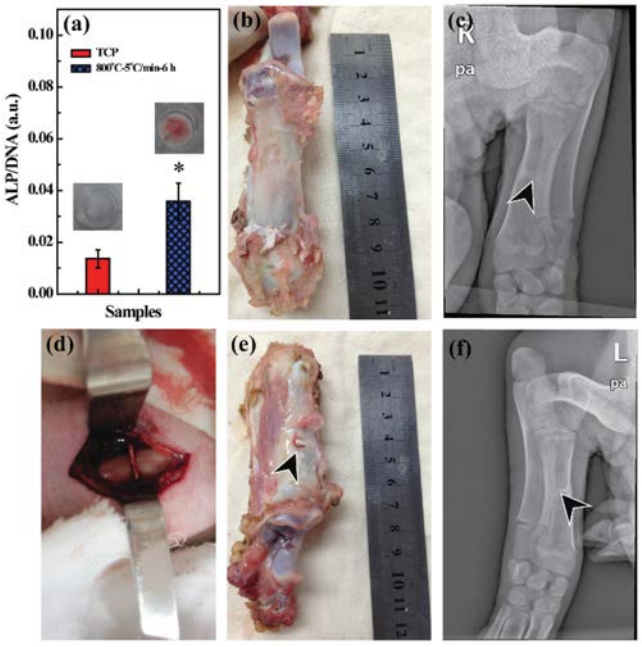

Figure 5. In vitro osteogenic differentiation of rat mesenchymal stem cells (MSCs) and in vivo bone repair. a) Alkaline phosphatase (ALP) activity of rMSCs cultured onto different substrates in growth medium after 14 days culture. Insert of (a) shows the picture of alizarin red staining of rMSCs cultured onto TCP (left) and LAP ceramic (right) in growth medium without any inducing factors at day 14. Panels (b–f) show the macroscopic appearance of bone defects; a 2 mm bone defect was created in the middle of the tibia, and implanted with laponite ceramic (d). Panels (b & e) show the macroscopic appearance of defects without and with implantation during 24 weeks. A trace of laponite ceramic residual is observed in (e) as pointed by the arrow. Panels (c & f) show the radiographic images of bone defects without and with LAP implantation after 24 weeks. Reproduced with permission.[33]

(TCP). In vivo healing of an induced bone defect was achieved by implantation of LAP ceramic into the damaged tibia of a rat (Figure 5b-f).

LAP nanodiscs in bone tissue engineering were further developed by their incorporation into a gelatin hydrogel to induce osteogenesis,[81] and as haemostatic agents.[82] These studies illustrated the excellent properties of LAP-based materials to induce bone formation.

Overall, tissue and bone engineering studies of 2DMs are still limited. There is certainly a need to explore more in this field using 2DMs.

4. Bioimaging

Over the past two decades, the advances of nanotechnology have allowed the development of new tools for bioimaging and diagnosis. Inorganic QDs have been largely explored due to their optical and semiconducting properties, high quantum yields, broad absorption spectra, tuneable dimensions, and strong resistance to photo-bleaching, becoming better candidates over organic fluorophores.[94] Although inorganic QDs seem to be the promising materials for diagnostic applications, the presence of heavy metals (e.g., Cd or Zn) have raised important toxicity concerns, limiting their potential for clinical translation. Recently, graphene-based QDs, devoid of metal atoms, have been developed. Even if these materials resulted in equally good signals for imaging, they suffer from poor photo-responsiveness and inherent hydrophobicity.[95] 2DMs also seem to be suitable candidates for bioimaging and diagnosis due to their tuneable large band-gaps (especially for MoS_2, WS_2, and g-C_3N_4) along with strong excitonic and fluorescence properties.

4.1. Fluorescence-Based Imaging

One of the first examples of bioimaging applications reported the use of water-dispersed exfoliated g-C_3N_4 nanosheets. The materials were biocompatible and exhibited a pH-dependent photoluminescence (PL) along with high quantum yield allowing efficient imaging within HeLa cells (**Figure 6**).[96] In addition to g-C_3N_4, MoS_2 sheets have been explored for bioimaging. Strongly fluorescent MoS_2 sheets of lateral dimension around 100 nm were found to exhibit stronger PL compared to larger sheets due to quantum size effect,[97] and were imaged within U251 glioblastoma cells. QDs from MoS_2 or WS_2 were also highly dispersible in aqueous phases and with strong fluorescence[98] compared to monolayered MoS_2 sheets,[97] and were imaged within HeLa and HEK293 cells. Apart from these few examples of in vitro studies, the in vivo imaging of these nanomaterials exploiting their intrinsic fluorescence is still unexplored. Studies in this direction would allow better understanding of the efficiency of g-C_3N_4 in comparison to other nanomaterials or organic dyes.

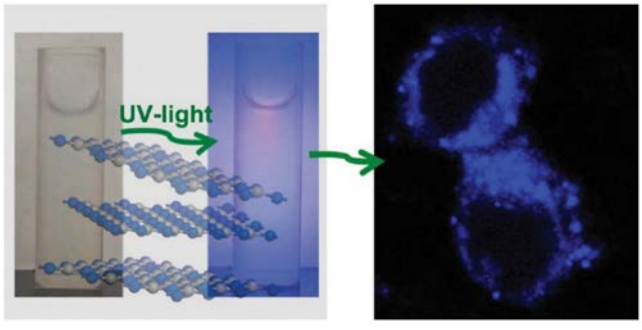

Figure 6. Exfoliation of g-C_3N_4 nanosheets in aqueous media and bioimaging of HeLa cells (right-hand panel). Reproduced with permission.[96] Copyright 2015, American Chemical Society.

4.2. X-ray Computed Tomography Imaging

X-ray computed tomography (CT) imaging is a well-established biomedical imaging technique being routinely used in clinical diagnosis.[99] CT is a non-invasive imaging technique which offers a 3D visual reconstruction and segmentation of the targeted tissues, deep tissue penetration at high resolution. In CT imaging, the weakening of incident X-rays is enhanced by agents that adsorb these irradiations, thereby providing image contrast.[100] Various nanoparticles have been explored as X-ray contrast agents consisting of lanthanide complexes of gadolinium, dysprosium, and ytterbium including, iodine, gold, bismuth, tantalum oxide (Ta_2O_5) and more recently graphene.[99,101]

2DMs like MoS_2, WS_2, Bi_2S_3 and Bi_2Se_3 can attenuate X-rays stronger than carbon-based materials, resulting in very promising contrast agents.[8,36,52,102] The strong contrast of X-rays created by MoS_2 sheets was superior to graphene and it was applied for CT imaging and image-guided therapy.[36] In an alternative work, strong X-ray attenuation ability was achieved using PEGylated WS_2 sheets (**Figure 7**a).[100] In this study, the dual-modality imaging of tumours through enhanced CT and photoacoustic tomography (PAT) (vide infra) was demonstrated. The contrast agent efficiency of PEGylated WS_2 increased linearly with the concentration of the conjugate (Figure 7b). Signal strength for the PEGylated WS_2 was found to be much higher than that of commercially available iopromide (currently clinically used) and also higher than that of MoS_2 sheets because of the stronger X-ray attenuation ability of W over Mo atoms.[36] CT imaging of tumours was performed after injecting of PEGylated WS_2 intratumorally (i.t.) or intravenously (i.v.) into Balb/c mice (Figure 7c and d). This study confirmed that PEGylated WS_2 nanosheets can offer strong X-ray attenuation for high-contrast CT imaging to visualize tumours. In a similar approach, WS_2 was coated with BSA and demonstrated to be again superior in contrast to iopromide.[69] Bi_2Se_3 and Bi_2S_3 nanoplatelets were also used as efficient contrast agents in CT imaging, since Bi is a metal with high atomic number (Z = 83).[12] Subsequently, various Bi-containing 2DMs were developed for imaging.[102–104]

4.3. Photoacoustic Tomography Imaging

PAT is an emerging modality in biomedical imaging. PAT allows image reconstruction at multiple scales and multiple contrast spectra in living species ranging from cellular organelles to entire organs.[105] This technique can also overcome

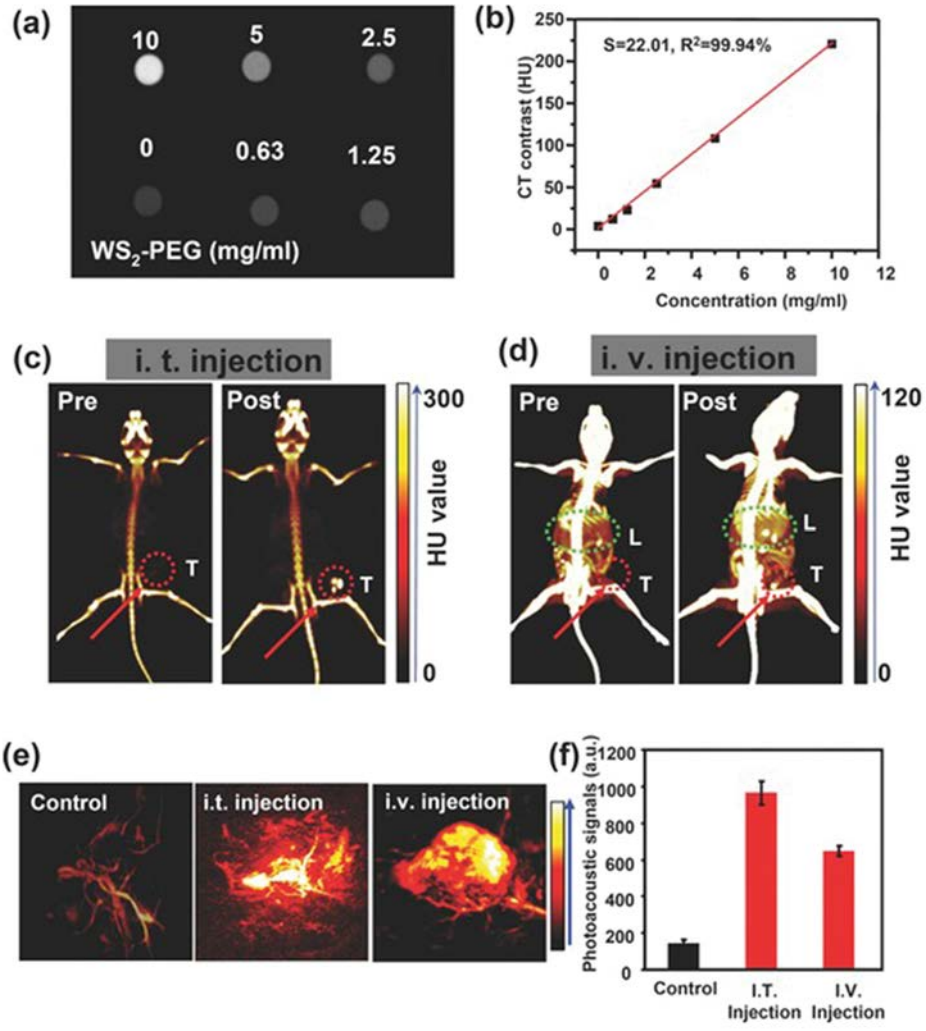

Figure 7. In vivo dual-modality imaging in 4T1-tumour-bearing mice. a) CT images of WS_2-PEG solutions at different concentrations. b) Hounsfield unit (HU) values of WS_2-PEG as the function of concentration. c) CT images of mice before and after intratumoral (i.t.) injection with WS_2-PEG (5 mg/mL, 20 μL). d) CT images of mice before and after intravenous (i.v.) injection with WS_2-PEG (5 mg/mL, 200 μL). CT contrast was enhanced in the mouse liver (green dashed circle) and tumour (red dashed circle). e) PAT images of tumours on mice before and after i.t. or i.v. injection with WS_2-PEG. f) Photoacoustic signals in the tumours from mice before and after i.t. or i.v. injections of WS_2-PEG solution. For PAT imaging, 20 and 200 μL of WS_2-PEG at the concentration of 2 mg/mL were i.t. or i.v. administrated, respectively. Reproduced with permission.[100] Copyright 2011, Wiley-VCH Verlag.

the scattering of optical photons in the tissues by utilizing the photoacoustic effect of light-absorbers, and it offers a remarkable increase of imaging in depth and higher spatial resolution compared to classical in vivo optical imaging.[100,105] The photoacoustic effect is based on the generation of acoustic waves by a material due to its ability for light absorption.[105,106] When endogenous molecules (such as haemoglobin, melanin, and water) fail to provide PAT imaging with high resolution, contrast agents can be administered.

Different nanomaterials like metallic nanoparticles,[107,108] CNTs[109] and graphene[106,110] have been used as contrast agents for PAT and used to map the lymphatic system, engineered tissues and brain.[106] PAT has been combined with CT to visualise the tumours in Balb/c mice after administration of PEGylated WS_2 nanosheets,[100] utilising its high NIR light absorption. After i.t. or i.v. injection of PEGylated WS_2, strong photoacoustic signals were recorded in the tumours under NIR laser irradiation (Figure 7e and f). PEGylated WS_2 have been described to result in better contrast signals for PAT imaging than graphene-based materials.[110] Similarly, PEGylated MoS_2 and TiS_2 have also been used as PAT contrast agents.[111,112] More recently, 2D PEGylated MoS_2/Bi_2S_3 hybrid nanosheets have been successfully synthesised by introducing bismuth ions to react with the S atoms of $(NH_4)_2MoS_4$, the precursor molecule for MoS_2.This hybrid material performed as a platform for both CT and PAT imaging.[113] Since Bi offers excellent X-ray attenuation ability, integration of Bi_2S_3 nanoparticles onto MoS_2 provided more sensitive CT and PAT imaging. This multimodal imaging has been successfully applied during NIR photothermal therapy for tumour treatment in mice models.[113]

Table 2. Representative multimodal therapies combined to imaging applications of 2DMs.

Material	Functionalisation/ Coating	Therapeutic/imaging molecules/NPs	Modalities	In vitro	In vivo	Route	Ref.
MoS_2	LA-PEG6-Amino-PEG	Fe_3O_4 NPs^{64}Cu	PTT, MRI/PET/PAT	–	Mice	i.v.	[15]
WS_2	LA-PEG	–	PTT, PAT/CT	–	Mice	i.t & i.v.	[100]
TiS_2	C_{18}-PMH-PEG	–	PTT, PAT	4T1	Mice	i.v.	[112]
MoS_2	Chitosan	Dox	Chemotherapy and PTT, X-ray CT	KB cells PA-1 cells	Mice	i.t.	[36]
MoS_2	PLGA	Dox	Chemotherapy and PTT, PAT	4T1	Mice	i.t.	[115]
Co_9Se_8	Polyacrylic acid (PAA)	Dox	Chemotherapy and PTT, PAT/MRI	HepG2	Mice	i.v.	[114]
g-C_3N_4	–	Dox	Chemotherapy and PDT, PL imaging	HeLa	–	–	[26]
g- C_3N_4	Mesoporous SiO_2 shell	Dox	Chemotherapy and PDT, two-photon imaging/MRI	A549	–	–	[116]
	PEG	Fe_3O_4 NPs RGD peptide		HeLa			
WS_2	BSA	PS methylene blue	PTT and PDT X-ray CT	HeLa	Mice	i.t.	[69]
WS_2	Gd^{3+}-doped PEG	–	PTT and RT X-ray CT/PAT/MRI	–	Mice	i.v.	[66]
MnO_2	PEG	Dox	Chemotherapy, MRI	MCF-7/ADR	Mice	i.t.	[117]
MnO_2	UCNPs	–	PDT/radiotherapy, PAT and UCL imaging	4T1	Mice	i.t. & i.v.	[118]

In addition to Mo, W and Ti dichalcogenide-based 2DMs, more recently cobalt chalcogenides were also explored for imaging purposes. Cobalt selenide (Co_9Se_8) sheets functionalised with poly(acrylic acid) (PAA) were exploited for PAT and MR dual-modal imaging.[114] Overall, the presence of heavy elements like Mo, W, Bi, and Ti render 2DMs more powerful contrast agents, especially for CT and PAT imaging, than graphene-based nanomaterials. Thus, tissue imaging can be improved with the use of these 2DMs in comparison to commercially available contrast agents.

5. Cancer Theranostics

2DMs are also promising materials for the design of combinatory therapeutics and for theranostics. Due to the intrinsic properties that have been evidenced by previous studies, the possibilities to use 2DMs as platforms for chemo- and photothermal therapies, multimodal imaging and their different combinations have inspired recent works (**Table 2**). Transition-metal dichalcogenides are among the most explored materials, with nanosheets of MoS_2, WS_2, and TiS_2 at the center of interesting studies.

5.1. Imaging Guided Photothermal Therapy

Following PEGylation of MoS_2 nanosheets, this material was used to prepare a new complex multimodal system.[15] MoS_2 was combined with superparamagnetic iron oxide (IO) nanoparticles for magnetic resonance imaging (MRI). Two PEGs [(d)PEG)] were added to stabilise the complexes in physiological conditions. Finally, radioactive ^{64}Cu was adsorbed to MoS_2 due to the high affinity of copper for sulphur that allows a chelating agent-free radiolabelling for positron emission tomography (PET). T_2-weighted MRI of MoS_2-IO-(d)PEG evidenced a concentration-dependent darkening effect, confirming the capability of this system as efficient T_2-contrast agents for MRI. These strong NIR responsive, radioactive and superparamagnetic complexes can be also used for PAT, due to high contrast and deep tissue penetration of ultrasound offered by the 2DMs and the nanoparticles (**Figure 8**). This triple modal imaging strategy combined to photothermal therapy was applied to tumour-bearing mice. Following systemic administration, high accumulation of the complexes into the tumour was observed using either PET, MRI or PAT. Subsequent laser irradiation at 808 nm led to a complete elimination of the tumours proving the remarkable efficacy of this advanced theranostic system.

The same strategy has been also applied to another type of transition metal dichalcogenide, namely WS_2.[100] The material has been PEGylated and used in vivo for photothermal therapy combined with imaging (Figure 7e and f). Mice were treated intratumorally or intravenously and irradiation using NIR light induced tumour ablation in both cases. Equivalent results were obtained replacing W with Ti.[112] TiS_2 stabilised with PEG and intravenously injected to tumour-bearing mice underwent photothermal activation leading to complete tumour regression. PAT allowed the detection of the 2DM that accumulated at the tumour site.

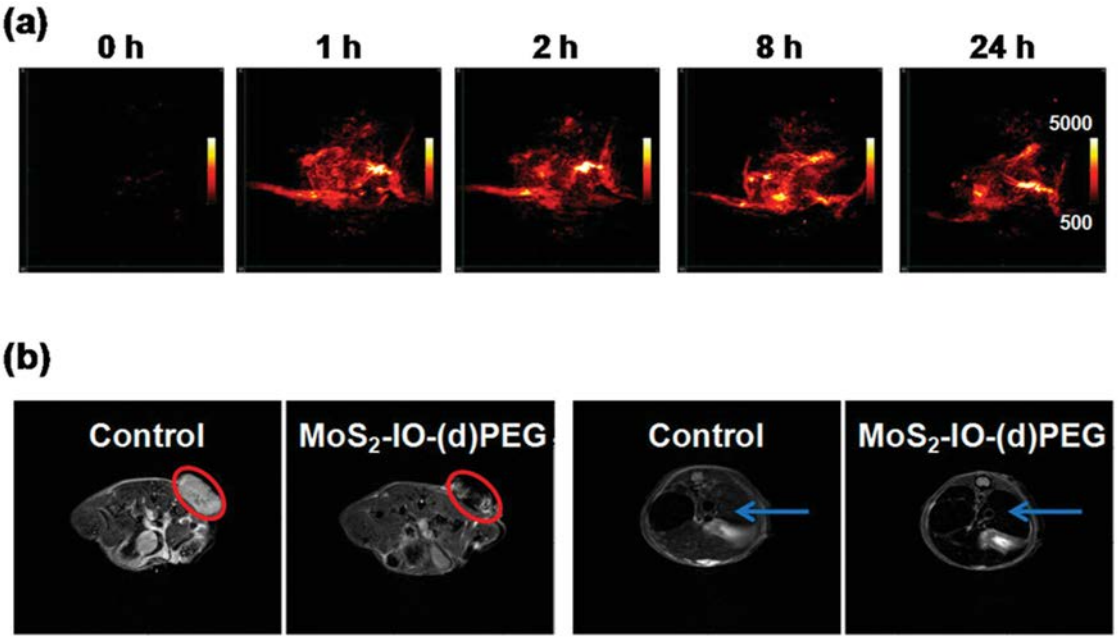

Figure 8. In vivo PAT and MRI. (a) PAT images of 4T1 tumour in mice at various time points after intravenous injection with MoS_2-IO-(d) PEG. (b) T_2-weighted MR images showing the transverse sections of a tumour-bearing mouse before and after injection with MoS_2-IO-(d)PEG. The red circles and blue arrows highlight the 4T1 tumour and liver of mice, respectively.Reproduced with permission.[15] Copyright 2015, American Chemical Society.

5.2. Imaging Guided Chemo- and Photothermal Therapy

Single layer MoS_2 nanosheets have been recently proposed for this purpose.[36] Exfoliated MoS_2 have been first functionalised with chitosan to improve their biocompatibility. The conjugates were then loaded with Dox (**Figure 9**). Controlled release of the drug was attained by irradiating the solution at 808 nm. The MoS_2 complexes were then used to treat cancer cells and tumour-bearing mice. The combination of the treatment resulted in a better synergistic effect than the chemotherapy or phototherapy applied separately, with complete regression of the pancreatic tumour model reported. The same system was also exploited in the same study as theranostic tool because MoS_2 nanosheets are efficient contrast agents for X-ray CT imaging.

Very recently, an injectable multifunctional composite constituted of PLGA, MoS_2 and Dox has been proposed.[115] It was characterised by the fast liquid/solid transition behavior of PLGA that allowed an easy intratumoral administration followed by a rapid solidification in the body fluid. NIR laser irradiation of the solidified implant triggered the release of Dox leading to complete tumour regression. The in vivo localisation of the composite was assessed by PAT imaging. As PLGA matrix cannot enter into the blood circulation, this system is potentially endowed of a better safety profile.

Since the transition metals and dichalcogenides offer many possible chemical combinations, very recently cobalt and selenium were combined to form nanoplates with Co_9Se_8 molecular composition, functionalised by polyacrylic acids and complexed with Dox.[114] After intratumoral administration, tumour growth was significantly reduced by the synergistic effect of the anticancer drug combined with irradiation in the NIR region. PAT imaging was combined to MRI, thanks to the large saturation magnetisation of cobalt, to observe the material into the tumour. The advantage of this 2DM likely resides on the intrinsic magnetic properties of the metal present in the form of clusters that make it an efficient T_2-weighted contrast agent for MRI.

5.3. Imaging Guided Chemo- and Photodynamic Therapy

Alternative 2DMs are represented by the forms that do not contain metals but they are constituted of carbon and nitrogen atoms. It is the case of graphitic C_3N_4 nanosheets.[26] This material is photoluminescent and therefore it can be imaged inside the cells. A complex based on g-C_3N_4 has been loaded with Dox and delivered to HeLa cells. A double therapeutic strategy, exploiting the release of the anticancer drug at low pH inside cancer cells and the capability of g-C_3N_4 to generate ROS, led to a dose-dependent cytotoxic effect comparable to free Dox. Although there was not a real gain in the anticancer activity, the use of this type of carrier can overcome disadvantages of using Dox alone. In addition, g-C_3N_4 could be detected inside the cells when excited at 405 nm indicating their use as bioimaging agents.

Very recently g-C_3N_4 has also been integrated in a more sophisticated system.[116] The proposed multifunctional nanocarrier is based on g-C_3N_4 decorated with iron oxide nanoparticles and coated with mesoporous silica shells. Mesoporous silica is able to impart additional properties to the complex. It can better stabilise the 2DM in physiological conditions, be further functionalised and its porosity is beneficial for the incorporation of a drug. A PEG chain with a cyclic RGD targeting peptide was added to the silica surface. Dox was then efficiently adsorbed into the silica channels and onto

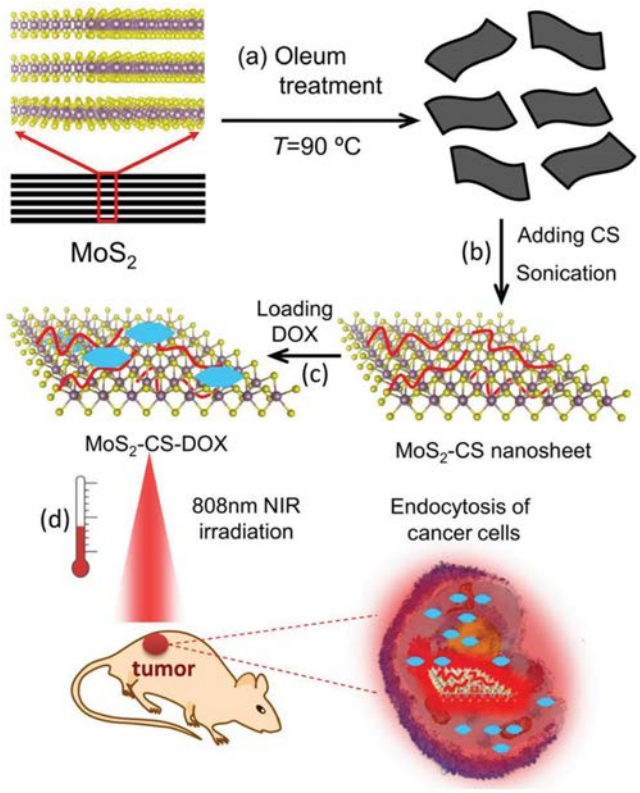

Figure 9. Illustration of the synthesis of MoS_2-chitosan nanosheets as a NIR photothermal triggered drug delivery system for efficient cancer therapy. (a,b) Oleum treatment exfoliation process to produce single layer MoS_2 nanosheets subsequently modified with chitosan (CS); (c) Dox loading; and (d) NIR photothermal-triggered drug delivery of the MoS_2 nanosheets to the tumour site. Reproduced with permission.[36] Copyright 2014, American Chemical Society.

g-C_3N_4 nanosheets. The conjugate was used to treat two types of cancer cells. A549 and HeLa cells were magnetically (by iron oxide nanoparticles) and chemically (by RGD peptide) targeted and underwent a synergistic chemotherapeutic (pH-triggered Dox release) and photodynamic (ROS generation under visible light) effect, leading to high percentage of cell death. In addition, cell imaging of the material was possible due to the autofluorescence of g-C_3N_4 that can be exploited for one- or two-photon detection modes.

5.4. Imaging Guided Photothermal, Photodynamic and Radiotherapy

The versatility of WS_2 for combined therapies has been further proven by preparing a different complex stabilised in water by BSA and coated with a photosensitiser (PS).[69] This conjugate has been used for a combined photodynamic and photothermal therapy (**Figure 10**). PS methylene blue was adsorbed on BSA-WS_2 and the therapeutic efficacy irradiating HeLa cells at 808 nm (for photothermal therapy) and at 665 nm (for photodynamic therapy) was superior to the modalities applied separately, again confirming the presence of a synergistic effect like in the examples previously described. The system was also used as contrast agent for CT allowing in vivo imaging after intratumoral injection.

Another complementary multimodal anticancer therapy was proposed very recently using Gd^{3+} doped-WS_2 nanosheets using a solution phase bottom-up preparation approach.[66] PEG functionalised WS_2 sheets containing gadolinium were utilised for in vivo treatment of tumour-bearing mice by a combined photothermal and radiation therapy under tri-modal (CT, PAT and MRI) image guidance. The doping of Gd^{3+} ions enhanced the contrast of WS_2 sheets in CT imaging as well as in MRI.

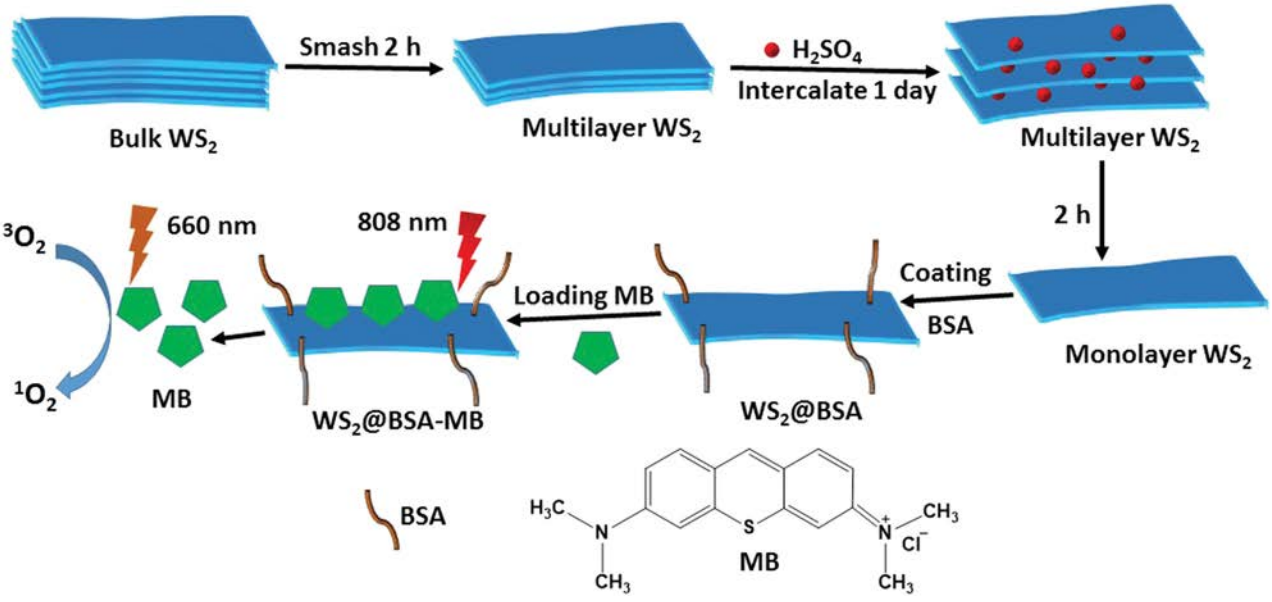

Figure 10. Illustration of the synthetic procedure to obtain WS_2 nanosheets coated with BSA and loaded with PS methylene blue, and their application as a multifunctional PS delivery system for combined photothermal and photodynamic therapy of cancer. Reproduced with permission.[69] Copyright 2014, the Royal Society of Chemistry.

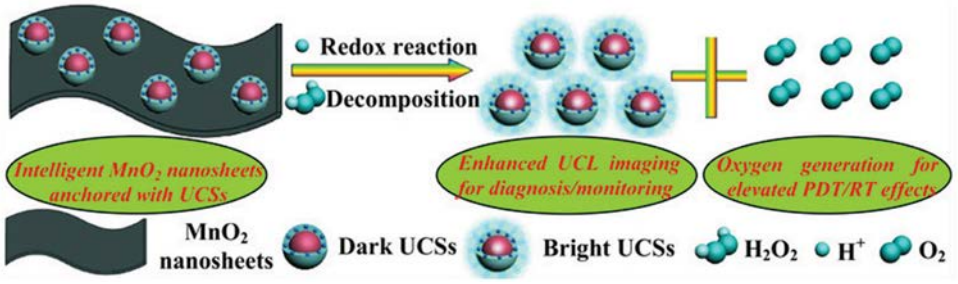

Figure 11. Schematic illustration of the decomposition of MnO_2 nanosheets arising from the redox reaction between UCSs and acidic H_2O_2, which leads to the enhanced UCL imaging for diagnosis/monitoring as well as the massive oxygen generation for improving the synergetic PDT/radiotherapy effects. Reproduced with permission.[118] Copyright 2015, Wiley-VCH Verlag.

Gd^{3+} ions also boosted the efficacy of radiation therapy treatment in vivo by the enhanced ionization in cancer cells.

Recent studies also exploited 2D transition metal oxides for biomedical applications including drug delivery, photothermal therapy, bioimaging and biosensing.[8] These transition metal oxides (e.g., MnO_2, TiO_2, etc.) are attracting increasing interest due to their pH/redox properties along with good biocompatibility. In particular, MnO_2 can decompose into Mn^{2+} ions in acidic pH environments and its paramagnetic character can be used for enhanced MRI. MnO_2 proved more suitable as T_1-contrast agent than gadolinium due to its higher biocompatibility.[8,119] Based on the unique pH-sensitive redox properties of MnO_2, an intelligent theranostic platform of PEG modified MnO_2 nanosheets with simultaneous ultrasensitive pH-responsive MRI and drug delivery was developed.[117] The pH-dependent release and in vivo imaging of tumour tissues was demonstrated by i.t. injection of PEG-MnO_2 conjugate into nude mice. Shi and co-workers used the pH-responsive redox properties of MnO_2 to design a smart nanosheet anchored with upconversion nanoparticles (UCSs) to generate a pH/H_2O_2 responsive nanoprobe for synergistic tumour therapy along with upconversion luminescent (UCL) image guidance.[118] These hybrid MnO_2/UCS sheets react with H_2O_2 generated in the tumour environment, thereby producing adequate oxygen species for enhancing the synergistic radio- and photodynamic therapy upon NIR light/X-ray irradiation. At the same time, the UCL helps to monitor the therapeutic process (**Figure 11**). The UCSs provide a high-resolution UCL with minimal autofluorescence and superior photostability, that can be used for imaging guidance during multimodal therapies.[120]

In view of the available studies, 2DMs look very promising as platforms for multimodal delivery. In particular, transition metal and chalcogenides offer a wide variety of atomic combinations, so theoretically can be expanded to diverse combination of materials for different biomedical applications. On the other hand, their properties appear very similar and it would therefore be more challenging to select one specific material over another.

6. Biosensing

Bioimaging is a very important diagnostic technique that spans verious fields of applications, including medical diagnosis, drug discovery, forensics, environmental monitoring and food safety. Indeed, there is a continuous demand for the development of highly sensitive, selective, more efficient and cost effective biosensing platforms.[28,121–123] Over the last two decades several nanomaterial-based biosensors have been developed due to their unique chemical, physical, electrical and optical properties including tuneable morphology and dimensions, mainly using gold NPs,[124] QDs[125] and CNTs.[126] The discovery of graphene has further generated lot of interest in the development of highly efficient sensors.[127] Especially, the high electron mobility across graphene sheets facilitates potentially high selectivity and accurate detection of biomolecules.[53] 2D graphene-based materials have high surface-to-volume ratio making them particularly sensitive to environmental changes. However, graphene-based sensing platforms, due to their zero band-gap, can result in increased current leakage leading to reduced sensitivity. Meanwhile, the emerging 2DMs such as MoS_2, MnO_2 and g-C_3N_4 have shown large band-gap compared to graphene that can be tuned between semiconductor or insulator states controllably,[27] preventing current leakage and allowing high sensitivity.[28] In addition, these materials are also endowed with fluorescence, electrical conductivity, fast heterogeneous electron transfer and high density of electronic states, leading to superior biosensing properties.[128,129] Representative biosensing applications of 2DMs are shown in the **Table 3**.

TMDCs can be used as transducing platforms or electroactive labels for the fabrication of biosensors.[146] The presence of adsorbed molecules on the monolayer surface of TMDCs will affect their electronic properties. The changes can be detected electrically by connecting TMDCs into a transistor and measuring the current–voltage trends, or optically by measuring the photoluminescence, absorbance or Raman spectra.[128,147] The changes in the photoluminescence of MoS_2 monolayer have been found useful in sensing stable fluorescent markers important for imaging and for fluorometric assays. A transistor made of few-layer MoS_2 was able to detect NO.[148] Alternatively, glassy carbon electrodes modified with reduced MoS_2 sheets showed sensitivity towards glucose and dopamine in the presence of ascorbic acid and uric acid.[130] The intrinsic PL of MoS_2 sheets have also been applied for developing an in situ sensor for glucose, where PL of MoS_2 sheets was controlled by the intercalation/deintercalation of K^+ and H^+ ions.[131] In the first model, the MoS_2-glucose oxidase (GOx) system was used to detect different concentrations of glucose at externally applied voltages lower than -1.0 V. In the second model, the changes in the PL

Table 3. Different types of biosensing applications of 2DMs.

Material	Analyte	Method of sensing	Ref.
Reduced MoS_2 sheets	Dopamine, glucose	Electrochemical	[130]
MoS_2 sheets	Glucose, yeast cells viability	Photoluminescence	[131]
MoS_2 sheets	pH, protein	FET-based sensing	[27]
MoS_2 sheets	DNA, small molecules	Fluorescence quenching	[28]
WS_2 sheets	DNA	Fluorescence quenching	[132]
WS_2 sheets	microRNA	Fluorescence quenching	[133]
MnO_2 sheets-carbon dots	Glutathione	FRET-based sensing	[134]
MnO_2-nanosheet with UCNPs	Glutathione	FRET-based sensing	[135]
MnO_2-5-carboxyfluorescein	microRNA and thrombin	FRET-based sensing	[136]
MnO_2 sheets with UCNPs	Ochratoxin A and cathepsin D	FRET-based sensing	[137]
MnO_2 sheets with 7-hydroxycoumarin	Ascorbic acid	FRET based sensing	[138]
MnO_2 sheets coated on persistent luminescence NPs	Glutathione in vivo	FRET without in situ light exposure	[139]
MnO_2-nanosheet modified- UCNPs	Glucose, hydrogen peroxide	FRET-based sensing	[140]
g-C_3N_4 nanosheet–MnO_2	Intracellular glutathione	FRET-based sensing	[25]
g-C_3N_4 sheets	Cu (II) ions	Photoinduced electron transfer aligned with DNA, metal ions, protein	[154]
g-C_3N_4 sheets	DNA, metal ions, protein		[142]
Fe doped g-C_3N_4 sheets	Glucose	Calorimetric	[141]
Au doped g-C_3N_4 sheets	Carcinoembryonic antigen	Electrochemiluminescence	[24]
Ag doped g-C_3N_4 sheets		Electrochemiluminescence	[143]
Perylenetetracarboxylic acid/g-C_3N_4 sheets	Dopamine	Electrochemiluminescence	[144]
Au NPs/g-C_3N_4 sheets	T4-polynucleotide kinase activity	Photoelectrochemical sensing	[145]

of MoS_2 were used to monitor the viability of yeast cells, where PL of quasi-2D MoS_2 sheets was utilized for investigating ion exchanges in cells (**Figure 12**). The dead cells do not suppress PL of MoS_2 since K^+ ions cannot intercalate without the help of driving forces, which occur only in viable cells, resulting in the generation of an electric field throughout the yeast membrane by transfer of K^+ ions across the membrane, leading to intercalation of K^+ ions into 2D MoS_2 sheets to suppress the fluorescence.

Because of their electrical and optical properties, 2DMs are better candidates than silicon nanowires and CNTs for constructing field-effect transistor (FET)-based biosensors. In general FET sensors are attractive since they offer rapid, cost-effective and label-free sensing platforms.[12,149,150] By utilising the semiconductor nature of MoS_2 nanosheets a FET-based biosensor with high sensitivity and easy patternability has been recently developed.[27] This sensing platform showed very high sensitivity from pH 3 to 9 and allowed detection of specific

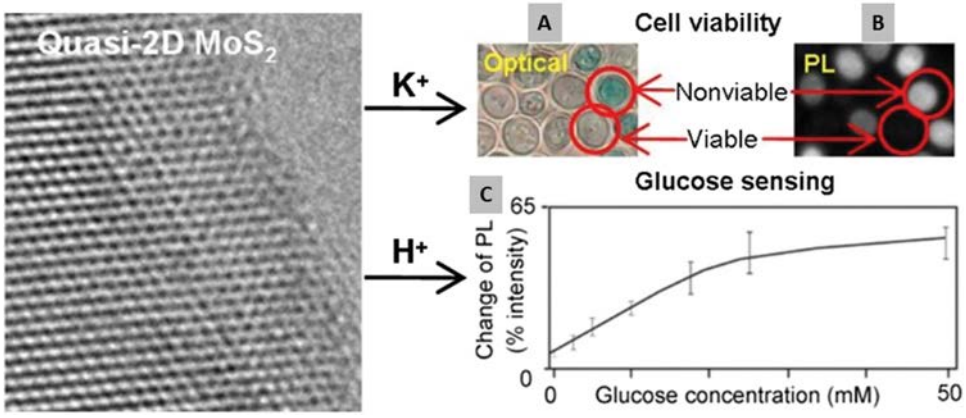

Figure 12. MoS_2 sheets and their usage as glucose sensor and viability sensors of yeast cells by recording the changes MoS_2 PL.[131] The left panel shows high resolution TEM image of quasi-2D MoS_2. Characterisation of the quasi-2D MoS_2–yeast cell system: (A) optical image of quasi-2D MoS_2 sheets coated with viable and non-viable yeast cells stained with Trypan blue, and (B) the corresponding PL image where viable cells are stained blue while dead cells lack of blue staining. Characterisation of the quasi-2D MoS_2–GOx system: Graphics (C) shows the PL modulation of the system at an applied voltage of –1.5 V and at different glucose concentrations. Reproduced with permission.[131] Copyright 2015, American Chemical Society.

proteins with ultra-sensitivity even at femtomolar concentration. This work highlights the advantage of the large band-gap of MoS_2 (1.9 eV) compared to graphene by comparing their sensitivity for detection of specific proteins.

Recently, a nanoprobe to detect DNA and small molecules based on the fluorescence quenching ability of single-layer MoS_2 has been fabricated. The fluorescence quenching efficiency varied depending on the single-stranded DNA (ssDNA) or double-stranded DNA (dsDNA) tagged with a fluorescent dye.[146] This method was successfully applied to detect adenosine within a few minutes. Similar to MoS_2, WS_2 sheets were also used to develop efficient DNA biosensors based on fluorescence quenching.[132] Upon interaction with other biomolecules (e.g., aptamers or peptides) the complexation between WS_2 sheets and ssDNA was altered, leading to recovery of fluorescence via the combined effect of excited-state energy transfer and a static quenching process. WS_2 sheets showed unique differential affinity towards short oligonucleotide fragments, thus becoming interesting tools to detect microRNA in the femtomolar range.[133] Most TMDC-based biosensors are using organic dyes (e.g., dye-modified ssDNA), however the latter often suffer from photobleaching and chemical instability. Therefore, there is a need to replace these organic molecules as energy donors.[134]

Similar to TMDCs, TMDOs have also excellent light absorption capabilities and fast electron transfer rates along with fluorescence quenching abilities. These characteristics render them interesting materials for fluorescence resonance energy transfer (FRET)-based chemical and biosensing applications.[135] FRET involves the non-radiative energy transfer from a luminescent donor to an energy acceptor at close distance (e.g., 1–10 nm). In particular, MnO_2 nanosheets have been applied in the fabrication of biosensors due to their high biocompatibility, redox activity and wide absorption band.[135,136] An efficient FRET biosensor for the intracellular detection of glutathione by coating of MnO_2 nanosheets with up-conversion lanthanide nanoparticles (UCNPs) has been proposed.[135] The UCNPs efficiently convert NIR light into visible light, resulting in a good alternative to organic fluorophores due to their high photostability.[135] MnO_2 nanosheets coated with UCNPs induced the quenching of NP luminescence that could be again turned on in the presence of glutathione due to the reduction of MnO_2 into Mn^{2+}. A few more FRET biosensors based on MnO_2 sheets were conceived in combination with UCNPs, or variations using luminescent NPs or carbon dots to detect ascorbic acid,[137,138] glutathione,[25,134,139] microRNA[136] and glucose.[140]

Some promising types of biosensors were also reported by exploiting the semiconducting properties of g-C_3N_4.[151] Compared to the bulk material, g-C_3N_4 monolayers have great photo- and electro-responsiveness due to their large surface area.[152,153] A highly efficient sensor using g-C_3N_4 nanosheets was developed, with the fluorescence of g-C_3N_4 quenched upon binding to Cu^{+2} ions via photo-induced electron transfer.[154] Sensing of copper ions is very important both biologically and environmentally. Similar to MoS_2, the fluorescence quenching property of g-C_3N_4 was also utilised to develop DNA biosensors.[142] Recently, multifunctional g-C_3N_4 nanosheets functionalised with folate and different dye-ssDNAs were used for in situ monitoring of intracellular miRNAs.[23] An interesting report using Fe-doped g-C_3N_4 nanosheets showed that peroxidase-activity could be mimicked by these sheets. This technique is simple and rapid, with high-selectivity in detection of glucose at low concentrations.[141] Furthermore, an immunosensor was developed using g-C_3N_4 nanosheets modified with the noble metal NPs to detect the carcinoembryonic antigen.[24,143,144] More recently, another photoelectrochemical biosensor has been constructed based on Au NP-decorated g-C_3N_4 for monitoring of T4 polynucleotide kinase activity.[145] The results obtained revealed almost 100% enhancement in the photocurrent able to be detected due to the surface plasmon resonance-enhanced light harvesting property of Au NPs/g-C_3N_4.

Overall, 2D materials (e.g., MoS_2, MnO_2 and g-C_3N_4) endowed of inherent semiconducting properties are promising for the development of high-efficient and cost-effective biosensing platforms for both in vitro and in vivo applications. In addition, their high biocompatibility and fast heterogeneous electron transfer properties propel them as better alternative to graphene in biosensing. It can be also anticipated that 2D materials may be used for developing a single device for detection of multiple targets in a simple and efficient manner.

7. Antimicrobials

Various 2DMs have been explored for their potential antibacterial activity following different strategies (**Table 4**). These include: i) coated surfaces with layered materials; ii) combination of 2DMs with antibacterial drugs for controlled release and enhancement of drug activity; or iii) exploitation of the intrinsic antibacterial capacity of the material itself.

Antibacterial coating and anti-biofouling are extremely important in clinical environments when the diffusion and growing of microorganisms is very high. The search for novel coating materials is very important to overcome the problem of bacterial resistance. Towards this direction, multi-layered films formed by titanium nanosheets (TNS) intercalated with lysozyme (LSZ) which is a natural antibacterial agent, have been designed and fabricated.[155] The modified surfaces with TNS/LSZ were evaluated against *Micrococcus lysodeikticus*, an organism sensitive to LSZ. Inactivation of bacteria was achieved either in the dark or under UV irradiation (**Figure 13**). TNS displayed antibacterial activity also in the absence of LSZ, but only under UV light. The presence of TNS in combination with the protein is fundamental as this material leads to an enhancement of cell killing by photoactivation. Both components of the film acted in a synergistic manner to exert high antibacterial activity against *M. lysodeikticus*. As this strategy can be easily implemented, it could be extended to the preparation of different films comprising other types of antibacterial agents.

Antibiotics can also be combined with 2DMs in an alternative approach. For example cephalosporin has been incorporated into a layered double hydroxide composed of zinc and aluminium.[156] The drug is chemically stabilised by the LDH layers by electrostatic interaction and released in a controlled manner. This resulted as an efficient delivery system of the antibacterial drug molecules leading to high inhibition of *S. aureus* proliferation. A similar system was developed by intercalating

Table 4. Antimicrobial properties of 2DMs.

Material	Combination with drugs or metals	Strategy	Type of microorganism	Antimicrobial activity and mechanism of action	Ref.
Titania nanosheets	Lysozyme	Layer-by-layer coating	*Micrococcus lysodeikticus*	Photoactivated antibacterial activity UV light inactivation ROS generation Lyzozyme autolysis of bacteria	[155]
Layered Zn-Al hydroxide	Cephalosporin	Addition of a dispersion to bacterial culture	*S. aureus*	Mechanism not reported Inhibition of bacterial proliferation Efficient release of cephalosporin in 0.8% NaCl	[156]
Layered Mg-Al hydroxide	Sodium benzoate Sodium succinate Benzylpenicillin Ticarcillin	Addition of a dispersion to bacterial culture	*Micrococcus lysodeikticus*	Enhanced ion exchange Release of the antibiotics Growth inhibition measured as a function of release of antibiotics	[157]
Zn-Ti LDH	Ti^{3+} generated in situ	Addition of LDHs to bacteria under visible light	*S. cerevisiae*, *S. aureus* or *E. coli*	LDH size effect and generation of $O_2^{\bullet-}$ radicals by Ti^{3+} under visible light	[158]
LAP- PLGA nanofibers	Amoxicillin	Addition of AMX-LAP-PLGA fibers to bacteria culture	*S. aureus*	Release of the antibiotics	[34]
LAP	Si(IV) phthalocyanine	Addition of LAP to bacteria culture	*S. aureus*	Generation of $^1O_2$ by 610 nm light exposure	[35]
Ultrathin	Ag nanoparticles	Addition of a dispersion to bacterial culture	*E. coli*	Visible light inactivation ROS production	[159]
g-C_3N_4			*S. aureus*	Oxidation of bacterial DNA, proteins and polysaccharides	
Chemically exfoliated MoS_2	–	Addition of a dispersion to bacterial culture	*E. coli*	Production of ROS Superoxide anion ($O_2^{\bullet-}$) production Induction of membrane and oxidation stress Glutathione oxidation $O_2^{\bullet-}$ independent oxidation	[40]
Exfoliated MoS_2	EDTA	Addition of a dispersion to bacterial culture	*E. coli*	Superoxide anion ($O_2^{\bullet-}$) production Hydrogen peroxide production Glutathione oxidation	[4]

antibiotic organic anions like benzoate, succinate, benzylpenicillin and ticarcillin into magnesium/aluminium LDHs.[157] The activity of the antibiotics was attributed to their controlled release from the composite when the LDH systems were incubated in a solution rich in sodium chloride (i.e., 3.5% NaCl). These constructs suggested the use of LDH materials as active reservoirs encapsulating different types of antibiotic anions for anti-fouling coating and sustained drug release. Using an alternative strategy to the antimicrobial action of LDH drug conjugates, the photochemical activity of Zn-Ti LDH under visible light was applied to kill *S. cerevisiae, S. aureus* and *E. coli*.[158] In another study, amoxicillin (AMX) was encapsulated into LAP-doped PLGA nanofibers that displayed a sustained release of the drug. An improved antimicrobial activity against *S. aureus* and a higher cytocompatibility were shown by LAP-PLGA fibers compared to pure PLGA fibers.[34] Furthermore, LAP nanodiscs were used to encapsulate the hydrophobic and photocatalytic dye, Si(IV)-phthalocyanine (SiPc). SiPc-LAP nanodiscs demonstrated selective elimination of drug-resistant gram (+) *S. aureus* in the presence of gram (-) *E.coli* via the generation of $^1O_2$ under visible light.[35] This selectivity was attributed to the specific interaction of the nanodiscs with gram (+) bacteria.

The use of noble metal nanoparticles in combination with 2DMs represents as alternative to natural or synthetic antibiotics. These types of NPs are excellent electron acceptors and their photoactivation can enhance the formation of radical oxygen species. Silver nanoparticles have been complexed to g-C_3N_4 nanosheets.[159] The antibacterial activity of these

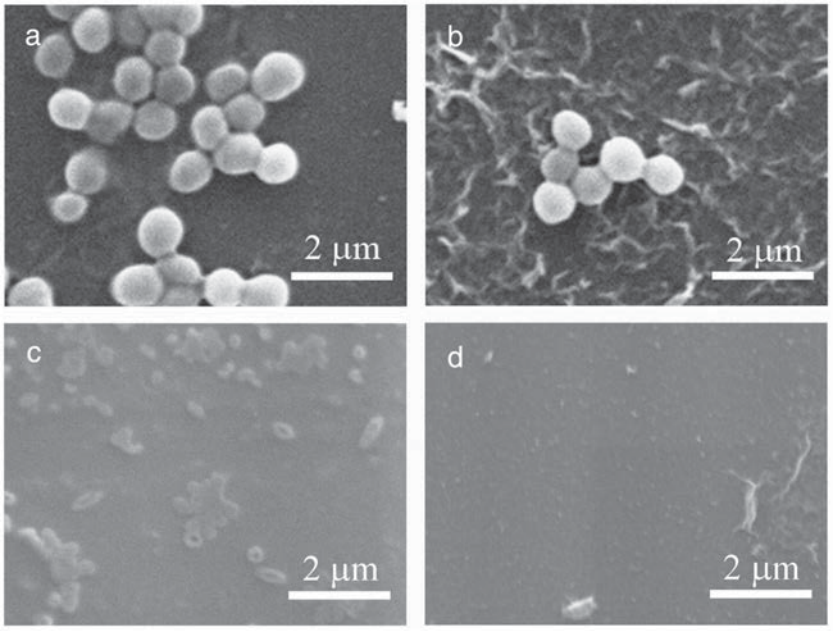

Figure 13. Scanning electron microscopy (SEM) images of *M. lysodeikticus* deposited on different surfaces: (a) uncoated quartz slide; (b) TNS film coated quartz slide; (c) and (d) TNS/LSZ film coated quartz slide. (a)-(c) Samples were treated in the absence of UV light; (d) sample was treated in the presence of UV light. Reproduced with permission.[155] Copyright 2012, Elsevier.

hybrids was assessed on *E. coli* and *S. aureus*. Both bacteria were inactivated under visible light (**Figure 14**). In addition, these complexes were able to disperse bacterial biofilms by oxidative damage of bacterial polysaccharides, DNA and proteins, the major components of the bacterial wall.

Similarly, hBN sheets modified with silver nanoparticles (hBN-Ag) were also studied for their antimicrobial activity, in comparison to hBN nanosheets functionalised with hydroxyl groups or polydopamine, against *S. aureus* and *E. coli* .[41] The results revealed that only hBN-Ag exerted significant antimicrobial activity, which was likely due to the presence of Ag nanoparticles. Such results may suggest that the antimicrobial activity of hBN sheets may be different to that of graphene sheets, whose activity is mediated by the physicochemical interactions of the sheets with the bacteria.[160] More detailed studies should offer better insight into the antimicrobial action of the hBN to develop efficiently antimicrobial coatings or surfaces based on these type of materials.

2DMs have also been described to exert some inherent antibacterial activity. Such inherent activity has been suggested in studies conducted previously using graphene oxide that reported some degree of antibacterial activity.[46,160–165] Chemically exfoliated MoS_2 was tested against *E. coli*[40] and some antibacterial activity was attributed to the high specific area of MoS_2 sheets. The particular 2DM was thought to be able to produce superoxide anions that could lead to membrane damage and oxidative stress on bacteria in closed contact with the surface, eventually inducing cell death. In particular, the mechanism of bacterial inactivation proposed involves the oxidation of glutathione (an important antioxidant in bacteria) by ROS, suggesting possible oxidation of bacterial components such as lipids, proteins and DNA, as shown for g-C_3N_4.[159] Similar results to that for *E. coli* were found in another report using exfoliated MoS_2 to study their antibacterial activity on planktonic cells and biofilms in the presence of ethylene diaminotetracetic acid (EDTA) as electron donor and under light activation.[4] The production of radical species and oxidation of glutathione were again seen enhanced.

The few available examples illustrate the potential development of 2DMs alone or in combination with antibiotics and nanoparticles as antibacterial coatings, anti-biofouling, anti-biofilm and antibacterial agents.

8. Toxicity Associated with 2DMs

The assessment of toxicity caused by 2DMs is still very poorly explored and understood. However, determination of risks associated with exposure to 2DMs is of fundamental importance for the translation of these new materials into clinical (or other) uses. Specific studies on cytotoxic responses have been mainly been associated to the development of 2DMs for

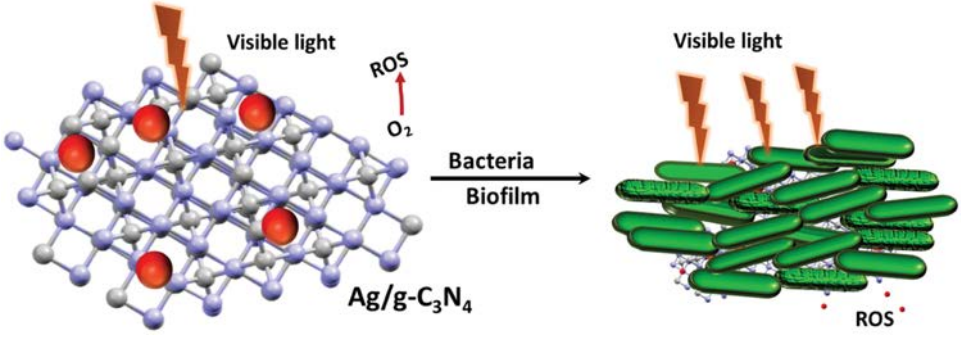

Figure 14. Schematic diagram showing the mechanism involved in the elimination of bacteria and biofilms by Ag/g-C_3N_4 complexes under visible light irradiation. Reproduced with permission.[159] Copyright 2015, Tsinghua University Press and Springer-Verlag Berlin, Heidelberg.

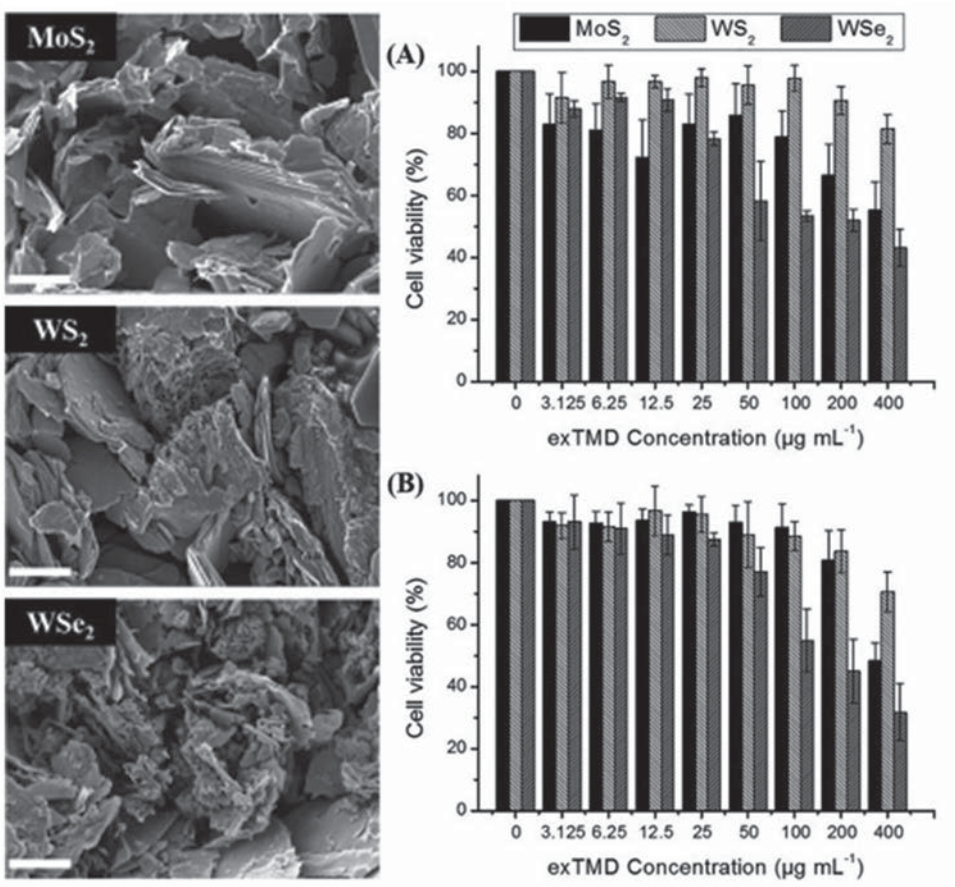

Figure 15. Nanosheets and their toxicity. (Left panels) SEM images of MoS_2, WS_2 and WSe_2 nanosheets (scale bars: 1 μm). (Right panels) Cell viability of human lung epithelial cells, measured with (A) MTT assay and (B) WST-8 assay, following 24 h exposure to varying amounts of exfoliated transition metal dichalcogenides (exTMDs). The percentages shown are normalized to unexposed control cells. Reproduced with permission.[166] Copyright 2014, Wiley-VCH Verlag.

therapeutic and imaging applications. Concerning layered double hydroxides, their toxic effects and biodistribution have been discussed in a recent comprehensive review.[32] This type of 2DMs can induce cytotoxic responses dependent on the dose, composition, size and shape of the material.

Limited studies on the cytotoxicity of transition metal dichalcogenides are available. In one study to assess the antimicrobial activity and the prevention of biofilm formation, exfoliated MoS_2 did not show significant cytotoxicity to mammalian fibroblasts.[4] No cell mortality was observed at the concentration of 100 ppm (1μg in 1,000,000 μg of solution) of exfoliated MoS_2, suggesting the relative low impact of this 2DM in vitro.

In a comparative study, the cytotoxic effects of different exfoliated transition metal dichalcogenide nanosheets, including MoS_2, WS_2 and WSe_2, were weighed against graphene analogues (**Figure 15**). Following 24 hour exposure at different doses, it was found that WS_2 induced the lowest cytotoxic effect in human lung carcinoma epithelial cells (A549), while the other 2DMs showed dose-dependent impact on cell viability, with WSe_2 being more toxic than MoS_2.[166] However, the validity of such data must be further investigated independently since the use of the MTT assay is known to suffer from significant interference, as evidenced repeatedly with other carbon nanomaterials.[167] It is imperative that extremely careful and systematic investigations should be undertaken to determine the appropriate assays, conditions and handling in order to assess cell viability devoid of false results.

Recent applications of MoS_2 nanosheets modified with chitosan and complexed with Dox resulted in biocompatible constructs, since in the absence of NIR irradiation neither significant cell mortality, nor haemolysis of RBCs were observed, encouraging their further development.[36] The absence of cytotoxic effects were confirmed on HeLa cells using MoS_2[70] and the effect on enzymatic activity of α-chymotrypsin was analysed to assess possible denaturing activity by MoS_2 via host-guest interactions. Although the enzyme activity was inhibited in a dose-dependent manner, this process was reversible by increasing the ionic strength, leading to restoration of enzymatic capacity and fully preserving the structure of the protein.

Low cytotoxic responses were confirmed in another study that used MoS_2 and PEGylated MoS_2 as drug carriers.[68] HeLa cell viability was moderately reduced only in the case of MoS_2, while no significant effect was observed for the PEGylated analogue even at high concentrations (i.e., 160 μg/mL). In this study the MTT assay was again used, but the production of ROS was also evaluated and remained unaltered, suggesting normal

induction of oxidative stress by both MoS_2 types. Similar results were also found for WS_2 and TS_2.[69,100,112] In addition, in vivo acute haemotoxicity was evaluated on MoS_2 measuring the blood parameters of injected mice up to 30 days. Only a reduction of alanine aminotransferase and the number of platelets were observed, although remaining within the physiological range.[68] Similar results (i.e., low in vitro and in vivo toxicity) were found for a more complex MoS_2 system very recently developed by the same authors.[15] More in vivo studies are necessary to determine any safety limitations of such material.

Very recently, a comprehensive analysis of pulmonary cytotoxic responses to three different types of MoS_2 samples described as "aggregated MoS_2 (Agg-MoS_2), MoS_2 exfoliated by lithiation (Lit-MoS_2), and MoS_2 dispersed by Pluronic F87 (PF87-MoS_2) has been reported.[37] No significant cytotoxic responses in THP-1 and BEAS-2B cell lines for all three samples were reported. However, Agg-MoS_2 showed strong pro-inflammatory and pro-fibrogenic responses in vitro, while the other two MoS_2 samples displayed negligible effects. Furthermore, an acute inflammation in the lungs of mice was induced by Agg-MoS_2, while PF87- and Lit-MoS_2 samples have shown almost no effect. A sub-chronic study (during 21 days post-exposure) did not evidence any pulmonary fibrosis with any of these forms of MoS_2. Interestingly, pluronic coating of MoS_2 sheets increased the dispersibility as well as biocompatibility of the material, by reducing the surface reactivity at the cellular and pulmonary interfaces. Overall, this study suggested the importance of exfoliation into single layers and surface functionalisation, since Agg-MoS_2 showed significant toxicity compared to exfoliated samples. Such results seem to be consistent and in line with the studies investigating cytotoxic responses to graphene-based material, where aggregated graphene sheets and platelets seem to be associated with higher risks compared to thin, closer to single layer material.[168]

Recently, electrical impedance spectroscopy was also used to assess the cytotoxic impact of MoS_2 sheets using rat pheochromocytoma (PC12) and rat adrenalmedulla endothelial (RAMEC) cell cultures.[38] Cell viability was only slightly affected in both types of cells, revealing that MoS_2 sheets have negligible effects. In a different study, the biocompatibility of MoS_2 nanoplatelets (8 nm thick) reinforced by PPF polymeric nanocomposites after crosslinking with *N*-vinyl pyrrolidone, using NIH3T3 fibroblasts and MC3T3 pre-osteoblasts was assessed.[79] The results suggested that the crosslinked nanocomposites showed high viability (78–100%), high cellular attachment (40–55%), and spreading. However, the degradation products of these hybrid composites showed modest toxicity that was due to degradation of PPF in the acidic medium.

Other types of metal-based 2DMs have also displayed low cytotoxicity. Ultra-small palladium nanosheets did not accumulate into major organs, were eliminated though the renal route and did not provoke organ damage or affect the body weight of tumour-bearing mice treated with photothermal therapy.[71] Similarly, boron nitride nanosheets modified with hydroxyl functions to render them highly dispersible in water have shown no cytotoxic effects on human fibroblasts or in prostate cancer cells in the absence of an anticancer drug, for the delivery of which they were explored.[22,169,170] Carbon and nitrogen-based 2DMs like g-C_3N_4 resulted also non-cytotoxic to cells at high doses (up to 300 μg/mL) suggesting them as a suitable alternative to transition or noble metal 2DMs.[26,116] Finally, the cytotoxicity of BP was evaluated.[171] A549 cells were treated with increasing concentrations of BP dispersions. A dose-dependent cytotoxicity was evidenced with cell mortality reaching about 50% at 50 μg/mL. However, the data should be considered with precaution as the two tetrazolium-based tests (WST-8 and MTT assays) showed high interference with the presence of BPs, particularly at the highest doses used (>100 μg/mL), leading to unreliable cytotoxic data.

9. Conclusions and Perspectives

In this review, we have provided an overview of the recent progress and achievements on the rapidly emerging area of biomedical applications using 2DMs. Currently, these materials are attracting intensive interdisciplinary attention, unveiling some very attractive optical and electronic properties, along with their diverse chemical compositions.[12] Though applications in biology are at their very early stage, several groups have attempted to exploit some distinct features of 2DMs for drug delivery, photothermal and synergistic therapeutics, biosensing, bioimaging, tissue engineering and antimicrobial coatings.[8] Although the applications of 2DMs in biomedicine are exciting, a lot more systematic investigation is necessary.[172]

It is clear from the different examples illustrated above that the physicochemical properties of 2DMs are driving their use in biomedicine. Semiconducting TMDCs and g-C_3N_4 including BP sheets are more promising for biosensing and NIR light-mediated photothermal therapy over other 2DMs. Electrically inert hBN sheets are more biocompatible and better suited for drug delivery and tissue engineering, although more thorough studies are still needed. On the other hand, even though hBN sheets resulted in reduced cytotoxic responses, the methods to produce stable aqueous dispersions are limited. This is because hBN possesses almost the same interlayer distance compared to graphene, even if B-N bond is dipolar compared to C-C bond.[41] Among 2DMs, g-C_3N_4 and BP look more advanced in the biomedical domain because of their higher water dispersibility and colloidal stability without the use of any surfactants or oxidation reactions. In the case of TMDCs, covalent functionalisation approaches on those sheets are still limited.[173] In addition, straightforward functionalisation methods need to be explored for hBN and BP sheets to make them better dispersible in water or physiological media. The development of new covalent functionalisations to produce highly water-soluble 2DMs to improve their biocompatibility and control their biodistribution will be an interesting area for future research. In this direction, novel syntheses of 2D materials for biomedical applications need to primarily concentrate on the control of their dimensions, surface functionalities, and aqueous dispersibility, since these parameters could critically determine the fate of 2DMs in physiological environments and in contact with biological matter.

Before translation of these nanomaterials into real uses, it is mandatory to check their impact on health and environment and to assess possible risk hazards. The same principles should be applied to all newly emerging 2DMs prior to their adoption in

various applications. Since the understanding of the properties of these new materials is still at the initial stage, only a very limited number of studies is dealing with in vitro and in vivo toxicity.[37] Hence, more detailed studies to understand the long term toxicity of each kind of the 2DMs is necessary. Some results such as those on cell activation and apoptosis should already provide information if 2DMs can be harmful or can be beneficial for cancer therapy. In this direction more systematic evaluations on various cell lines on the respective 2DMs should be done.[172]

The lessons learnt from biopersistence and environmental persistence of other nanomaterials should be also applied for the development of 2DMs.[48,172,174] Some of the toxicological studies on carbon-based materials have shown that CNTs and graphene can generate acute lung damages along with sub-chronic granulomatous inflammation and fibrosis.[168,175–180] Thus, these kinds of investigations should be performed with all 2DMs to assess their safety profile benchmarked against previous data. For example, a recent report described in vivo acute cytotoxicity of various MoS_2 sheets, and revealed that highly dispersible MoS_2 did not induce sub-chronic inflammatory effects in mice.[37] In terms of biodegradability, data are still missing. We could hypothesise that hBN sheets, with a greater resistance towards oxidation than graphene oxide, might be more difficult to degrade. Conversely, BP sheets have shown light-induced degradability by converting into biocompatible phosphorous oxides.[6] As this type of degradability is not present in the other 2DMs, BP might be more suited for biomedical applications.[31] Similar to CNTs and graphene,[92,181,182] 2DMs like g-C_3N_4 and TMDCs have an inherently semiconducting nature, that makes them interesting for applications in tissue engineering and regenerative medicine. Notably, BP sheets possess semiconducting and photoinduced degradability, and thus they could be promising material in these fields. In the case of 2D clay materials, laponite nanodiscs seem to be promising biomaterials. Due to their unique interlayer space, pH-responsiveness and colloidal stability, LAPs could be remarkable drug carriers. Since LAP nanodiscs resulted in biodegradable non-toxic products, therefore highly biocompatible in vivo, one should consider them as components of the next-generation drug delivery systems.[73]

The properties of 2DMs beyond graphene are distinct, thereby making them attractive as novel nanomaterials for various biomedical applications. Their tuneable band-gaps and versatile chemical composition along with the low cytotoxic responses so far observed are great advantages for biological applications. The current results are exciting and encouraging scientists to explore more these materials. One critical issue that will need to be addressed before clinical translation of any 2DMs as a biomedical tool is their long-term cytotoxic burden as well as their environmental persistence. We do not believe that there will be a single, ideal 2DM to be suitable for all types of biomedical applications; however, we can generalise that different types of 2DMs will be selected, optimised and further developed for specific purposes to provide solutions for specific clinical challenges.

Acknowledgements

This work was supported by the Center National de la Recherche Scientifique (CNRS), by the Agence Nationale de la Recherche (ANR) through the LabEx project Chemistry of Complex Systems (ANR-10-LABX-0026_CSC) and by the International Center for Frontier Research in Chemistry (icFRC). The authors gratefully acknowledge financial support from EU FP7-ICT-2013-FET-F GRAPHENE Flagship project (no. 604391). Authors also thank Dr. Ravula Thirupathi (University of Michigan) for his help in preparing some figures.
Note: The section numbering was corrected on August 3, 2016, after initial publication online.

Received: December 18, 2015
Published online: April 23, 2016

[1] A. Geim, K. Novoselov, *Nat. Mater.* **2007**, *6*, 183.
[2] G. Yang, C. Zhu, D. Du, J. Zhu, Y. Lin, *Nanoscale* **2015**, *7*, 14217.
[3] V. Nicolosi, M. Chhowalla, M. G. Kanatzidis, M. S. Strano, J. N. Coleman, *Science* **2013**, *340*, 1226419.
[4] J. Fan, Y. Li, H. N. Nguyen, Y. Yao, D. F. Rodrigues, *Environ. Sci.: Nano* **2015**, *2*, 370.
[5] S. Butler, S. Hollen, L. Cao, Y. Cui, J. Gupta, H. Gutierrez, T. Heinz, S. Hong, J. Huang, A. Ismach, E. Johnston-Halperin, M. Kuno, V. Plashnitsa, R. Robinson, R. Ruoff, S. Salahuddin, J. Shan, L. Shi, M. Spencer, M. Terrones, W. Windl, J. Goldberger, *ACS Nano* **2013**, *7*, 2898.
[6] H. Wang, X. Yang, W. Shao, S. Chen, J. Xie, X. Zhang, J. Wang, Y. Xie, *J. Am. Chem. Soc.* **2015**, *137*, 11376.
[7] S. Wang, Y. Wu, R. Guo, Y. Huang, S. Wen, M. Shen, J. Wang, X. Shi, *Langmuir* **2013**, *29*, 5030.
[8] K. Kalantar-zadeh, J. Z. Ou, T. Daeneke, M. S. Strano, M. Pumera, S. L. Gras, *Adv. Funct. Mater.* **2015**, *25*, 5086.
[9] O. Mashtalir, M. Naguib, V. N. Mochalin, Y. Dall'Agnese, M. Heon, M. W. Barsoum, Y. Gogotsi, *Nat. Commun.* **2013**, *4*, 1716.
[10] L. Cao, *MRS Bull.* **2015**, *40*, 592.
[11] D. Chimene, D. L. Alge, A. K. Gaharwar, *Adv. Mater.* **2015**, *27*, 7261.
[12] Y. Chen, C. Tan, H. Zhang, L. Wang, *Chem. Soc. Rev.* **2015**, *44*, 2681.
[13] M. Acerce, D. Voiry, M. Chhowalla, *Nat. Nanotechnol.* **2015**, *10*, 313.
[14] R. Lv, J. A. Robinson, R. E. Schaak, D. Sun, Y. Sun, T. E. Mallouk, M. Terrones, *Acc. Chem. Res.* **2014**, *48*, 56.
[15] T. Liu, S. Shi, C. Liang, S. Shen, L. Cheng, C. Wang, X. Song, S. Goel, T. E. Barnhart, W. Cai, Z. Liu, *ACS Nano* **2015**, *9*, 950.
[16] D. Lee, B. Lee, K. H. Park, H. J. Ryu, S. Jeon, S. H. Hong, *Nano Lett.* **2015**, *15*, 1238.
[17] P. Ma, J. Spencer, *J. Mater. Sci.* **2015**, *50*, 313.
[18] Z. Liu, Y. Gong, W. Zhou, L. Ma, J. Yu, J. C. Idrobo, J. Jung, A. H. MacDonald, R. Vajtai, J. Lou, P. M. Ajayan, *Nat. Commun.* **2013**, *4*, 1.
[19] L. H. Li, J. Cervenka, K. Watanabe, T. Taniguchi, Y. Chen, *ACS Nano* **2014**, *8*, 1457.
[20] Z. Kuang, Y. Chen, Y. Lu, L. Liu, S. Hu, S. Wen, Y. Mao, L. Zhang, *Small* **2015**, *11*, 1655.
[21] W. L. Song, P. Wang, L. Cao, A. Anderson, M. J. Meziani, A. J. Farr, Y. P. Sun, *Angew. Chem. Int. Ed.* **2012**, *51*, 6498.
[22] Q. Weng, B. Wang, X. Wang, N. Hanagata, X. Li, D. Liu, X. Wang, X. Jiang, Y. Bando, D. Golberg, *ACS Nano* **2014**, *8*, 6123.
[23] X. Liao, Q. Wang, H. Ju, *Chem. Commun.* **2014**, *50*, 13604.
[24] L. Chen, X. Zeng, P. Si, Y. Chen, Y. Chi, D.-H. Kim, G. Chen, *Anal. Chem.* **2014**, *86*, 4188.
[25] X.-L. Zhang, C. Zheng, S.-S. Guo, J. Li, H.-H. Yang, G. Chen, *Anal. Chem.* **2014**, *86*, 3426.
[26] L.-S. Lin, Z.-X. Cong, J. Li, K.-M. Ke, S.-S. Guo, H.-H. Yang, G.-N. Chen, *J. Mater. Chem. B* **2014**, *2*, 1031.
[27] D. Sarkar, W. Liu, X. Xie, A. C. Anselmo, S. Mitragotri, K. Banerjee, *ACS Nano* **2014**, *8*, 3992.
[28] C. Zhu, Z. Zeng, H. Li, F. Li, C. Fan, H. Zhang, *J. Am. Chem. Soc.* **2013**, *135*, 5998.

[29] V. Tran, R. Soklaski, Y. Liang, L. Yang, *Phys. Rev. B* **2014**, *89*, 235319.
[30] H. Liu, Y. Du, Y. Deng, P. D. Ye, *Chem. Soc. Rev.* **2015**, *44*, 2732.
[31] Z. Sun, H. Xie, S. Tang, X.-F. Yu, Z. Guo, J. Shao, H. Zhang, H. Huang, H. Wang, P. K. Chu, *Angew. Chem. Int. Ed.* **2015**, *54*, 11581.
[32] A. U. Kura, M. Z. Hussein, S. Fakurazi, P. Arulselvan, *Chem. Cent. J.* **2014**, *8*, 47.
[33] C. Wang, S. Wang, K. Li, Y. Ju, J. Li, Y. Zhang, J. Li, X. Liu, X. Shi, Q. Zhao, *PLoS ONE* **2014**, *9*, e99585.
[34] S. Wang, F. Zheng, Y. Huang, Y. Fang, M. Shen, M. Zhu, X. Shi, *ACS Appl. Mater. Interfaces* **2012**, *4*, 6393.
[35] M. Grüner, L. Tuchscherr, B. Löffler, D. Gonnissen, K. Riehemann, M. C. Staniford, U. Kynast, C. A. Strassert, *ACS Appl. Mater. Interfaces* **2015**, *7*, 20965.
[36] W. Yin, L. Yan, J. Yu, G. Tian, L. Zhou, X. Zheng, X. Zhang, Y. Yong, J. Li, Z. Gu, Y. Zhao, *ACS Nano* **2014**, *8*, 6922.
[37] X. Wang, N. D. Mansukhani, L. M. Guiney, Z. Ji, C. H. Chang, M. Wang, Y.-P. Liao, T.-B. Song, B. Sun, R. Li, T. Xia, M. C. Hersam, A. E. Nel, *Small* **2015**, *11*, 5079.
[38] S. Pratikkumar, N. N. Tharangattu, L. Chen-Zhong, A. Subbiah, *Nanotechnology* **2015**, *26*, 315102.
[39] S. Wang, K. Li, Y. Chen, H. Chen, M. Ma, J. Feng, Q. Zhao, J. Shi, *Biomaterials* **2015**, *39*, 206.
[40] X. Yang, J. Li, T. Liang, C. Ma, Y. Zhang, H. Chen, N. Hanagata, H. Su, M. Xu, *Nanoscale* **2014**, *6*, 10126.
[41] R. A. Kumer, P. Byoungnam, L. K. Seok, P. S. Young, I. Insik, *Nanotechnology* **2014**, *25*, 445603.
[42] Y. Zhang, D. Petibone, Y. Xu, M. Mahmood, A. Karmakar, D. Casciano, S. Ali, A. S. Biris, *Drug Metab. Rev.* **2014**, *46*, 232.
[43] S. Goenka, V. Sant, S. Sant, *J. Control. Release* **2014**, *173*, 75.
[44] K. Yang, L. Feng, X. Shi, Z. Liu, *Chem. Soc. Rev.* **2013**, *42*, 530.
[45] C. Xu, J. Wang, Y. Xu, G. Shang, R. Wang, Y. Lin, *Curr. Drug Metab.* **2013**, *14*, 863.
[46] H. Y. Mao, S. Laurent, W. Chen, O. Akhavan, M. Imani, A. A. Ashkarran, M. Mahmoudi, *Chem. Rev.* **2013**, *113*, 3407.
[47] C. Chung, Y.-K. Kim, D. Shin, S.-R. Ryoo, B. H. Hong, D.-H. Min, *Acc. Chem. Res.* **2013**, *46*, 2211.
[48] C. Bussy, H. Ali-Boucetta, K. Kostarelos, *Acc. Chem. Res.* **2013**, *46*, 692.
[49] J. Bartelmess, S. J. Quinn, S. Giordani, *Chem. Soc. Rev.* **2015**, *44*, 4672.
[50] P. T. Yin, S. Shah, M. Chhowalla, K.-B. Lee, *Chem. Rev.* **2015**, *115*, 2483.
[51] F. Perreault, A. F. de Faria, M. Elimelech, *Chem. Soc. Rev.* **2015**, *44*, 5861.
[52] J. M. Yoo, J. H. Kang, B. H. Hong, *Chem. Soc. Rev.* **2015**, *44*, 4835.
[53] K. V. Krishna, C. Ménard-Moyon, S. Verma, A. Bianco, *Nanomedicine* **2013**, *8*, 1669.
[54] A. Bianco, *Angew. Chem. Int. Ed.* **2013**, *52*, 4986.
[55] D. L. A. D. Chimene, A. K. Gaharwar, *Adv. Mater.* **2015**, *27*, 7261.
[56] M. Xu, T. Liang, M. Shi, H. Chen, *Chem. Rev.* **2013**, *113*, 3766.
[57] X. Li, H. Zhu, *J. Materiomics* **2015**, *1*, 33.
[58] J. Coleman, M. Lotya, A. O'Neill, S. Bergin, P. King, U. Khan, K. Young, A. Gaucher, S. De, R. Smith, I. Shvets, S. Arora, G. Stanton, H.-Y. Kim, K. Lee, G. Kim, G. Duesberg, T. Hallam, J. Boland, J. Wang, J. Donegan, J. Grunlan, G. Moriarty, A. Shmeliov, R. Nicholls, J. Perkins, E. Grieveson, K. Theuwissen, D. McComb, P. Nellist, *Science* **2011**, *331*, 568.
[59] S. S. Chou, M. De, J. Kim, S. Byun, C. Dykstra, J. Yu, J. Huang, V. P. Dravid, *J. Am. Chem. Soc.* **2013**, *135*, 4584.
[60] C. Y. Zhi, Y. Bando, T. Terao, C. C. Tang, H. Kuwahara, D. Golberg, *Chem Asian J* **2009**, *4*, 1536.
[61] T. Sainsbury, A. Satti, P. May, Z. Wang, I. McGovern, Y. K. Gun'ko, J. Coleman, *J. Am. Chem. Soc.* **2012**, *134*, 18758.
[62] Y. Lin, T. V. Williams, W. Cao, H. E. Elsayed-Ali, J. W. Connell, *J. Phys. Chem. C* **2010**, *114*, 17434.
[63] S. Presolski, M. Pumera, *Mater. Today* **2015**, http://dx.doi.org/10.1016/j.mattod.2015.08.019.
[64] Z. Cui, A. J. Oyer, A. J. Glover, H. C. Schniepp, D. H. Adamson, *Small* **2014**, *10*, 2352.
[65] C. Tan, H. Zhang, *Nat. Commun.* **2015**, *6*, 1.
[66] L. Cheng, C. Yuan, S. Shen, X. Yi, H. Gong, K. Yang, Z. Liu, *ACS Nano* **2015**, *9*, 11090.
[67] C. Gautam, C. S. Tiwary, S. Jose, G. Brunetto, S. Ozden, S. Vinod, P. Raghavan, S. Biradar, D. S. Galvao, P. M. Ajayan, *ACS Nano* **2015**, *9*, 12088.
[68] T. Liu, C. Wang, X. Gu, H. Gong, L. Cheng, X. Shi, L. Feng, B. Sun, Z. Liu, *Adv. Mater.* **2014**, *26*, 3433.
[69] Y. Yong, L. Zhou, Z. Gu, L. Yan, G. Tian, X. Zheng, X. Liu, X. Zhang, J. Shi, W. Cong, W. Yin, Y. Zhao, *Nanoscale* **2014**, *6*, 10394.
[70] S. S. Chou, B. Kaehr, J. Kim, B. M. Foley, M. De, P. E. Hopkins, J. Huang, C. J. Brinker, V. P. Dravid, *Angew. Chem. Int. Ed.* **2013**, *52*, 4160.
[71] S. Tang, M. Chen, N. Zheng, *Small* **2014**, *10*, 3139.
[72] S.-J. Choi, G. E. Choi, J.-M. Oh, Y.-J. Oh, M.-C. Park, J.-H. Choy, *J. Mater. Chem.* **2010**, *20*, 9463.
[73] K. Li, S. Wang, S. Wen, Y. Tang, J. Li, X. Shi, Q. Zhao, *ACS Appl. Mater. Interfaces* **2014**, *6*, 12328.
[74] Y. Wu, R. Guo, S. Wen, M. Shen, M. Zhu, J. Wang, X. Shi, *J. Mater. Chem. B* **2014**, *2*, 7410.
[75] G. Chen, D. Li, J. Li, X. Cao, J. Wang, X. Shi, R. Guo, *New J. Chem.* **2015**, *39*, 2847.
[76] G. Wang, D. Maciel, Y. Wu, J. Rodrigues, X. Shi, Y. Yuan, C. Liu, H. Tomás, Y. Li, *ACS Appl. Mater. Interfaces* **2014**, *6*, 16687.
[77] D. Wang, N. Ge, J. Li, Y. Qiao, H. Zhu, X. Liu, *ACS Appl. Mater. Interfaces* **2015**, *7*, 7843.
[78] G. Lalwani, A. M. Henslee, B. Farshid, L. Lin, F. K. Kasper, Y.-X. Qin, A. G. Mikos, B. Sitharaman, *Biomacromolecules* **2013**, *14*, 900.
[79] B. Farshid, G. Lalwani, B. Sitharaman, *J. Biomed. Mater. Res. A* **2015**, *103*, 2309.
[80] S. Wang, R. Castro, X. An, C. Song, Y. Luo, M. Shen, H. Tomas, M. Zhu, X. Shi, *J. Mater. Chem.* **2012**, *22*, 23357.
[81] J. R. Xavier, T. Thakur, P. Desai, M. K. Jaiswal, N. Sears, E. Cosgriff-Hernandez, R. Kaunas, A. K. Gaharwar, *ACS Nano* **2015**, *9*, 3109.
[82] A. K. Gaharwar, R. K. Avery, A. Assmann, A. Paul, G. H. McKinley, A. Khademhosseini, B. D. Olsen, *ACS Nano* **2014**, *8*, 9833.
[83] W. Feng, L. Chen, M. Qin, X. Zhou, Q. Zhang, Y. Miao, K. Qiu, Y. Zhang, C. He, *Sci. Rep.* **2015**, *5*, 17422.
[84] R. W. Redmond, J. N. Gamlin, *Photochem. Photobiol.* **1999**, *70*, 391.
[85] Q. Wang, D. O'Hare, *Chem. Rev.* **2012**, *112*, 4124.
[86] A. C. S. Alcântara, P. Aranda, M. Darder, E. Ruiz-Hitzky, *J. Mater. Chem.* **2010**, *20*, 9495.
[87] Y. Kuthati, R. K. Kankala, C.-H. Lee, *Appl. Clay Sci.* **2015**, *112–113*, 100.
[88] Y.-M. Kuo, Y. Kuthati, R. K. Kankala, P.-R. Wei, C.-F. Weng, C.-L. Liu, P.-J. Sung, C.-Y. Mou, C.-H. Lee, *J. Mater. Chem. B* **2015**, *3*, 3447.
[89] J. K. Park, Y. B. Choy, J.-M. Oh, J. Y. Kim, S.-J. Hwang, J.-H. Choy, *Int. J. Pharm.* **2008**, *359*, 198.
[90] M. Gonçalves, P. Figueira, D. Maciel, J. Rodrigues, X. Shi, H. Tomás, Y. Li, *Macromol. Biosci.* **2014**, *14*, 110.
[91] K. Nagahama, D. Kawano, N. Oyama, A. Takemoto, T. Kumano, J. Kawakami, *Biomacromolecules* **2015**, *16*, 880.
[92] A. E. Jakus, E. B. Secor, A. L. Rutz, S. W. Jordan, M. C. Hersam, R. N. Shah, *ACS Nano* **2015**, *9*, 4636.

[93] C. Wu, J. Chang, J. Wang, S. Ni, W. Zhai, *Biomaterials* **2005**, *26*, 2925.
[94] J. Li, J.-J. Zhu, *Analyst* **2013**, *138*, 2506.
[95] O. S. Wolfbeis, *Chem. Soc. Rev.* **2015**, *44*, 4743.
[96] X. Zhang, X. Xie, H. Wang, J. Zhang, B. Pan, Y. Xie, *J. Am. Chem. Soc.* **2013**, *135*, 18.
[97] N. Wang, F. Wei, Y. Qi, H. Li, X. Lu, G. Zhao, Q. Xu, *ACS Appl. Mater. Interfaces* **2014**, *6*, 19888.
[98] S. Xu, D. Li, P. Wu, *Adv. Funct. Mater.* **2015**, *25*, 1127.
[99] H. Lusic, M. W. Grinstaff, *Chem. Rev.* **2013**, *113*, 1641.
[100] L. Cheng, J. Liu, X. Gu, H. Gong, X. Shi, T. Liu, C. Wang, X. Wang, G. Liu, H. Xing, W. Bu, B. Sun, Z. Liu, *Adv. Mater.* **2014**, *26*, 1886.
[101] K. Yang, S. Zhang, G. Zhang, X. Sun, S.-T. Lee, Z. Liu, *Nano Lett.* **2010**, *10*, 3318.
[102] J. Li, F. Jiang, B. Yang, X. R. Song, Y. Liu, H. H. Yang, D. R. Cao, W. R. Shi, G. N. Chen, *Sci. Rep.* **2013**, *3*, 1998.
[103] O. Rabin, J. Manuel Perez, J. Grimm, G. Wojtkiewicz, R. Weissleder, *Nat. Mater.* **2006**, *5*, 118.
[104] K. Ai, Y. Liu, J. Liu, Q. Yuan, Y. He, L. Lu, *Adv. Mater.* **2011**, *23*, 4886.
[105] L. V. Wang, S. Hu, *Science* **2012**, *335*, 1458.
[106] G. Lalwani, X. Cai, L. Nie, L. V. Wang, B. Sitharaman, *Photoacoustics* **2013**, *1*, 62.
[107] D. Pan, X. Cai, C. Yalaz, A. Senpan, K. Omanakuttan, S. A. Wickline, L. V. Wang, G. M. Lanza, *ACS Nano* **2012**, *6*, 1260.
[108] X. Cai, W. Li, C.-H. Kim, Y. Yuan, L. V. Wang, Y. Xia, *ACS Nano* **2011**, *5*, 9658.
[109] A. De La Zerda, C. Zavaleta, S. Keren, S. Vaithilingam, S. Bodapati, Z. Liu, J. Levi, B. R. Smith, T.-J. Ma, O. Oralkan, Z. Cheng, X. Chen, H. Dai, B. T. Khuri-Yakub, S. S. Gambhir, *Nat. Nanotechnol.* **2008**, *3*, 557.
[110] Z. Sheng, L. Song, J. Zheng, D. Hu, M. He, M. Zheng, G. Gao, P. Gong, P. Zhang, Y. Ma, L. Cai, *Biomaterials* **2013**, *34*, 5236.
[111] T. Liu, C. Wang, W. Cui, H. Gong, C. Liang, X. Shi, Z. Li, B. Sun, Z. Liu, *Nanoscale* **2014**, *6*, 11219.
[112] X. Qian, S. Shen, T. Liu, L. Cheng, Z. Liu, *Nanoscale* **2015**, *7*, 6380.
[113] S. Wang, X. Li, Y. Chen, X. Cai, H. Yao, W. Gao, Y. Zheng, X. An, J. Shi, H. Chen, *Adv. Mater.* **2015**, *27*, 2775.
[114] X.-R. Song, X. Wang, S.-X. Yu, J. Cao, S.-H. Li, J. Li, G. Liu, H.-H. Yang, X. Chen, *Adv. Mater.* **2015**, *27*, 3285.
[115] S. Wang, Y. Chen, X. Li, W. Gao, L. Zhang, J. Liu, Y. Zheng, H. Chen, J. Shi, *Adv. Mater.* **2015**, *27*, 7117.
[116] H. Wan, Y. Zhang, W. Zhang, H. Zou, *ACS Appl. Mater. Interfaces* **2015**, *7*, 9608.
[117] Y. Chen, D. Ye, M. Wu, H. Chen, L. Zhang, J. Shi, L. Wang, *Adv. Mater.* **2014**, *26*, 7019.
[118] W. Fan, W. Bu, B. Shen, Q. He, Z. Cui, Y. Liu, X. Zheng, K. Zhao, J. Shi, *Adv. Mater.* **2015**, *27*, 4155.
[119] Y. Chen, H. Chen, S. Zhang, F. Chen, S. Sun, Q. He, M. Ma, X. Wang, H. Wu, L. Zhang, L. Zhang, J. Shi, *Biomaterials* **2012**, *33*, 2388.
[120] G. Chen, H. Qiu, P. N. Prasad, X. Chen, *Chem. Rev.* **2014**, *114*, 5161.
[121] S. Rodriguez-Mozaz, M. Lopez de Alda, D. Barceló, *Anal. Bioanal. Chem.* **2006**, *386*, 1025.
[122] B. M. Paddle, *Biosens. Bioelectron.* **1996**, *11*, 1079.
[123] I. E. Tothill, *Semin. Cell Dev. Biol.* **2009**, *20*, 55.
[124] D. A. Giljohann, D. S. Seferos, W. L. Daniel, M. D. Massich, P. C. Patel, C. A. Mirkin, *Angew. Chem. Int. Ed.* **2010**, *49*, 3280.
[125] R. Gill, M. Zayats, I. Willner, *Angew. Chem. Int. Ed.* **2008**, *47*, 7602.
[126] W. Yang, K. R. Ratinac, S. P. Ringer, P. Thordarson, J. J. Gooding, F. Braet, *Angew. Chem. Int. Ed.* **2010**, *49*, 2114.
[127] T. Kuila, S. Bose, P. Khanra, A. K. Mishra, N. H. Kim, J. H. Lee, *Biosens. Bioelectron.* **2011**, *26*, 4637.
[128] Q. H. Wang, K. Kalantar-Zadeh, A. Kis, J. N. Coleman, M. S. Strano, *Nat. Nanotechnol.* **2012**, *7*, 699.
[129] M. Pumera, A. H. Loo, *TrAC, Trends Anal. Chem.* **2014**, *61*, 49.
[130] S. Wu, Z. Zeng, Q. He, Z. Wang, S. J. Wang, Y. Du, Z. Yin, X. Sun, W. Chen, H. Zhang, *Small* **2012**, *8*, 2264.
[131] J. Z. Ou, A. F. Chrimes, Y. Wang, S.-y. Tang, M. S. Strano, K. Kalantar-zadeh, *Nano Lett.* **2014**, *14*, 857.
[132] Y. Yuan, R. Li, Z. Liu, *Anal. Chem.* **2014**, *86*, 3610.
[133] Q. Xi, D.-M. Zhou, Y.-Y. Kan, J. Ge, Z.-K. Wu, R.-Q. Yu, J.-H. Jiang, *Anal. Chem.* **2014**, *86*, 1361.
[134] Y. Wang, K. Jiang, J. Zhu, L. Zhang, H. Lin, *Chem. Commun.* **2015**, *51*, 12748.
[135] R. Deng, X. Xie, M. Vendrell, Y.-T. Chang, X. Liu, *J. Am. Chem. Soc.* **2011**, *133*, 20168.
[136] C. Wang, W. Zhai, Y. Wang, P. Yu, L. Mao, *Analyst* **2015**, *140*, 4021.
[137] Y. Yuan, S. Wu, F. Shu, Z. Liu, *Chem. Commun.* **2014**, *50*, 1095.
[138] W. Zhai, C. Wang, P. Yu, Y. Wang, L. Mao, *Anal. Chem.* **2014**, *86*, 12206.
[139] N. Li, W. Diao, Y. Han, W. Pan, T. Zhang, B. Tang, *Chem. Eur. J.* **2014**, *20*, 16488.
[140] J. Yuan, Y. Cen, X.-J. Kong, S. Wu, C.-L. Liu, R.-Q. Yu, X. Chu, *ACS Appl. Mater. Interfaces* **2015**, *7*, 10548.
[141] J. Tian, Q. Liu, A. M. Asiri, A. H. Qusti, A. O. Al-Youbi, X. Sun, *Nanoscale* **2013**, *5*, 11604.
[142] Q. Wang, W. Wang, J. Lei, N. Xu, F. Gao, H. Ju, *Anal. Chem.* **2013**, *85*, 12182.
[143] X. Li, Z. Guo, J. Li, Y. Zhang, H. Ma, X. Pang, B. Du, Q. Wei, *Anal. Chim. Acta* **2015**, *854*, 40.
[144] X. Fu, J. Feng, X. Tan, Q. Lu, R. Yuan, S. Chen, *RSC Adv.* **2015**, *5*, 42698.
[145] J. Zhuang, W. Lai, M. Xu, Q. Zhou, D. Tang, *ACS Appl. Mater. Interfaces* **2015**, *7*, 8330.
[146] A. H. Loo, A. Bonanni, Z. Sofer, M. Pumera, *ChemPhysChem* **2015**, *16*, 2304.
[147] S. Balendhran, J. Z. Ou, M. Bhaskaran, S. Sriram, S. Ippolito, Z. Vasic, E. Kats, S. Bhargava, S. Zhuiykov, K. Kalantar-zadeh, *Nanoscale* **2012**, *4*, 461.
[148] H. Li, Z. Yin, Q. He, H. Li, X. Huang, G. Lu, D. W. H. Fam, A. I. Y. Tok, Q. Zhang, H. Zhang, *Small* **2012**, *8*, 63.
[149] F. Withers, H. Yang, L. Britnell, A. P. Rooney, E. Lewis, A. Felten, C. R. Woods, V. Sanchez Romaguera, T. Georgiou, A. Eckmann, Y. J. Kim, S. G. Yeates, S. J. Haigh, A. K. Geim, K. S. Novoselov, C. Casiraghi, *Nano Lett.* **2014**, *14*, 3987.
[150] X. Tong, E. Ashalley, F. Lin, H. Li, Z. Wang, *Nano-Micro Lett.* **2015**, *7*, 203.
[151] M. Rong, L. Lin, X. Song, T. Zhao, Y. Zhong, J. Yan, Y. Wang, X. Chen, *Anal. Chem.* **2015**, *87*, 1288.
[152] Q. Zhao, Y. Li, R. Liu, A. Chen, G. Zhang, F. Zhang, X. Fan, *J. Mate. Chem. A* **2013**, *1*, 15039.
[153] L. Chen, D. Huang, S. Ren, T. Dong, Y. Chi, G. Chen, *Nanoscale* **2013**, *5*, 225.
[154] J. Tian, Q. Liu, A. M. Asiri, A. O. Al-Youbi, X. Sun, *Anal. Chem.* **2013**, *85*, 5595.
[155] Y. Wang, D. Zhang, *Surf. Coat. Technol.* **2012**, *210*, 71.
[156] S.-J. Ryu, H. Jung, J.-M. Oh, J.-K. Lee, J.-H. Choy, *J. Phys. Chem. Solids* **2010**, *71*, 685.
[157] Y. Wang, D. Zhang, *Mater. Res. Bull.* **2012**, *47*, 3185.
[158] Y. Zhao, C. J. Wang, W. Gao, B. Li, Q. Wang, L. Zheng, M. Wei, D. G. Evans, X. Duan, D. O'Hare, *J. Mater. Chem. B* **2013**, *1*, 5988.
[159] W. Bing, Z. Chen, H. Sun, P. Shi, N. Gao, J. Ren, X. Qu, *Nano Res.* **2015**, *8*, 1648.

[160] F. Perreault, A. F. de Faria, S. Nejati, M. Elimelech, *ACS Nano* **2015**, *9*, 7226.
[161] M. Mahmoudi, O. Akhavan, M. Ghavami, F. Rezaee, S. M. A. Ghiasi, *Nanoscale* **2012**, *4*, 7322.
[162] O. Akhavan, E. Ghaderi, *ACS Nano* **2010**, *4*, 5731.
[163] V. T. H. Pham, V. K. Truong, M. D. J. Quinn, S. M. Notley, Y. Guo, V. A. Baulin, M. Al Kobaisi, R. J. Crawford, E. P. Ivanova, *ACS Nano* **2015**, *9*, 8458.
[164] A. F. de Faria, F. Perreault, E. Shaulsky, L. H. Arias Chavez, M. Elimelech, *ACS Appl. Mater. Interfaces* **2015**, *7*, 12751.
[165] S. Romero-Vargas Castrillón, F. Perreault, A. F. de Faria, M. Elimelech, *Environ. Sci. Technol. Lett.* **2015**, *2*, 112.
[166] W. Z. Teo, E. L. K. Chng, Z. Sofer, M. Pumera, *Chem. Eur. J.* **2014**, *20*, 9627.
[167] J. M. Wörle-Knirsch, K. Pulskamp, H. F. Krug, *Nano Lett.* **2006**, *6*, 1261.
[168] X. Wang, M. C. Duch, N. Mansukhani, Z. Ji, Y.-P. Liao, M. Wang, H. Zhang, B. Sun, C. H. Chang, R. Li, S. Lin, H. Meng, T. Xia, M. C. Hersam, A. E. Nel, *ACS Nano* **2015**, *9*, 3032.
[169] G. Ciofani, S. Danti, G. G. Genchi, B. Mazzolai, V. Mattoli, *Small* **2013**, *9*, 1672.
[170] L. Horváth, A. Magrez, D. Golberg, C. Zhi, Y. Bando, R. Smajda, E. Horváth, L. Forró, B. Schwaller, *ACS Nano* **2011**, *5*, 3800.
[171] N. M. Latiff, W. Z. Teo, Z. Sofer, A. C. Fisher, M. Pumera, *Chem. Eur. J.* **2015**, *21*, 13991.
[172] K. Kostarelos, K. S. Novoselov, *Science* **2014**, *344*, 261.
[173] D. Voiry, A. Goswami, R. Kappera, e. SilvaCecilia de Carvalho Castro, D. Kaplan, T. Fujita, M. Chen, T. Asefa, M. Chhowalla, *Nat. Chem.* **2015**, *7*, 45.
[174] K. Kostarelos, K. S. Novoselov, *Nat. Nanotechnol.* **2014**, *9*, 744.
[175] A. Erdely, M. Dahm, B. T. Chen, P. C. Zeidler-Erdely, J. E. Fernback, M. E. Birch, D. E. Evans, M. L. Kashon, J. A. Deddens, T. Hulderman, S. A. Bilgesu, L. Battelli, D. Schwegler-Berry, H. D. Leonard, W. McKinney, D. G. Frazer, J. M. Antonini, D. W. Porter, V. Castranova, M. K. Schubauer-Berigan, *Part. Fiber. Toxicol.* **2013**, *10*, 53.
[176] R. M. Silva, K. Doudrick, L. M. Franzi, C. TeeSy, D. S. Anderson, Z. Wu, S. Mitra, V. Vu, G. Dutrow, J. E. Evans, P. Westerhoff, L. S. Van Winkle, O. G. Raabe, K. E. Pinkerton, *ACS Nano* **2014**, *8*, 8911.
[177] A. A. Shvedova, E. Kisin, A. R. Murray, V. J. Johnson, O. Gorelik, S. Arepalli, A. F. Hubbs, R. R. Mercer, P. Keohavong, N. Sussman, J. Jin, J. Yin, S. Stone, B. T. Chen, G. Deye, A. Maynard, V. Castranova, P. A. Baron, V. E. Kagan, *Am. J. Physiol. Lung Cell Mol. Physiol.* **2008**, *295*, L552.
[178] A. B. Seabra, A. J. Paula, R. de Lima, O. L. Alves, N. Durán, *Chem. Res. Toxicol.* **2014**, *27*, 159.
[179] L. Ma-Hock, V. Strauss, S. Treumann, K. Küttler, W. Wohlleben, T. Hofmann, S. Gröters, K. Wiench, B. van Ravenzwaay, R. Landsiedel, *Part. Fiber. Toxicol.* **2013**, *10*, 23.
[180] A. Sasidharan, S. Swaroop, C. K. Koduri, C. M. Girish, P. Chandran, L. S. Panchakarla, V. H. Somasundaram, G. S. Gowd, S. Nair, M. Koyakutty, *Carbon* **2015**, *95*, 511.
[181] H. Porwal, S. Grasso, L. Cordero-Arias, C. Li, A. Boccaccini, M. Reece, *J. Mater. Sci. Mater. Med.* **2014**, *25*, 1403.
[182] C. Gaillard, G. Celiot, S. Li, F. M. Toma, H. Dumortier, G. Spaliuto, B. Cacciari, M. Prato, L. Ballerini, A. Bianco, *Adv. Mater.* **2009**, *21*, 2903.